Australian Journal of Earth Sciences (2007) **54**, (243–271)

Geochemistry and age of magmatic rocks in the unexposed Narromine, Cowal and Fairholme Igneous Complexes in the Ordovician Macquarie Arc, New South Wales

A. J. CRAWFORD[1]*, D. R. COOKE[1] AND C. M. FANNING[2]

[1]*ARC Centre of Excellence in Ore Deposits, School of Earth Sciences, University of Tasmania, Private Bag 79, Hobart, Tas. 7001, Australia.*
[2]*PRISE, Research School of Earth Sciences, Australian National University, ACT 0200, Australia.*

Much of the northern and southern sections of the Junee–Narromine Volcanic Belt of the Ordovician Macquarie Arc in central-western New South Wales are buried beneath the sediment cover of the Great Artesian Basin. Exploration drilling of these aeromagnetically defined blocks has provided important new material to assess the temporal and magmatic affinities of the rocks in the Narromine Igneous Complex (northern end) and the Cowal and Fairholme Igneous Complexes (southern end). Basement rocks are representative of Phase 1 magmatism in the Macquarie Arc, and consist of Lower Ordovician basalts and andesites and common volcaniclastic rocks, all with high-K calc-alkaline affinities. These are very similar compositionally to the Lower Ordovician Nelungaloo Volcanics that outcrop in the central part of the Junee–Narromine Volcanic Belt west of Parkes. Intruding the basement volcanic–volcaniclastic package are three distinct igneous suites. The oldest of these, dated at *ca* 466–460 Ma (Middle Ordovician) and representative of Phase 2 magmatism in the Macquarie Arc, consists of stocks of monzogabbro, monzodiorite and monzonite with high-K calc-alkaline affinities, and is well represented in the Narromine and Cowal Igneous Complexes. Phase 2 suite rocks were, in turn, intruded in the Bolindian (445 ± 5 Ma) by kilometre-size stocks, narrow sheets and dykes made up of hornblende gabbro, diorite and granodiorite, and including quartz + plagioclase +hornblende-phyric dacitic porphyries in the Narromine Igneous Complex. These medium-K calc-alkaline rocks, assigned to the Phase 3 Copper Hill Suite that also occurs in the Molong and Rockley–Gulgong Volcanic Belts further east, crystallised from andesitic or more evolved magmas, probably derived via partial melting of low-K rocks in the arc basement, or amphibolites in the subducting slab. The youngest rocks in these igneous complexes are believed to be the high-level shoshonitic intrusives in the Cowal and Fairholme Igneous Complexes, which are correlated on petrographic and compositional grounds with the Macquarie Arc Phase 4 (Bolindian and Llandovery) magmatic products best represented by the Northparkes Igneous Complex in the central part of the Junee–Narromine Volcanic Belt.

KEY WORDS: Cowal Igneous Complex, Fairholme Igneous Complex, geochemistry, geochronology, Macquarie arc, Narromine Igneous Complex.

INTRODUCTION

Geophysical data indicate that the Junee–Narromine Volcanic Belt (Figure 1) is the root section of the now disrupted Ordovician Macquarie Arc in central-western New South Wales (Direen *et al.* 2001). Large areas of the Junee–Narromine Volcanic Belt are buried beneath cover up to several hundred metres thick, with the only exposed section being the central part from Parkes, through the Forbes region, to the Gidginbung –Temora area (Lyons & Wallace 1999; Raymond & Sherwin 1999; Simpson *et al.* 2005; Crawford *et al.* 2007; Glen *et al.* 2007c). Much of the northern and southern extremities of this belt in New South Wales are unexposed, and are only known from exploration drilling in the Cowal and Fairholme (southern) and Narromine (northern) Igneous Complexes (Figure 1).

In this paper, we document the petrology, geochemistry and age relationships of Ordovician Macquarie Arc rocks, based on (petrographically determined) least-altered rocks sampled in drillcore from these unexposed complexes, and compare them with better-known sections of the Junee–Narromine Volcanic Belt to contribute to a more comprehensive knowledge of the tectono-magmatic development of both this belt, and the Macquarie Arc. Figure 2 gives a summary of key magmatic units and their ages in the three major igneous complexes that make up this study,

*Corresponding author: tony.crawford@utas.edu.au

ISSN 0812-0099 print/ISSN 1440-0952 online © 2007 Geological Society of Australia
DOI: 10.1080/08120090701221714

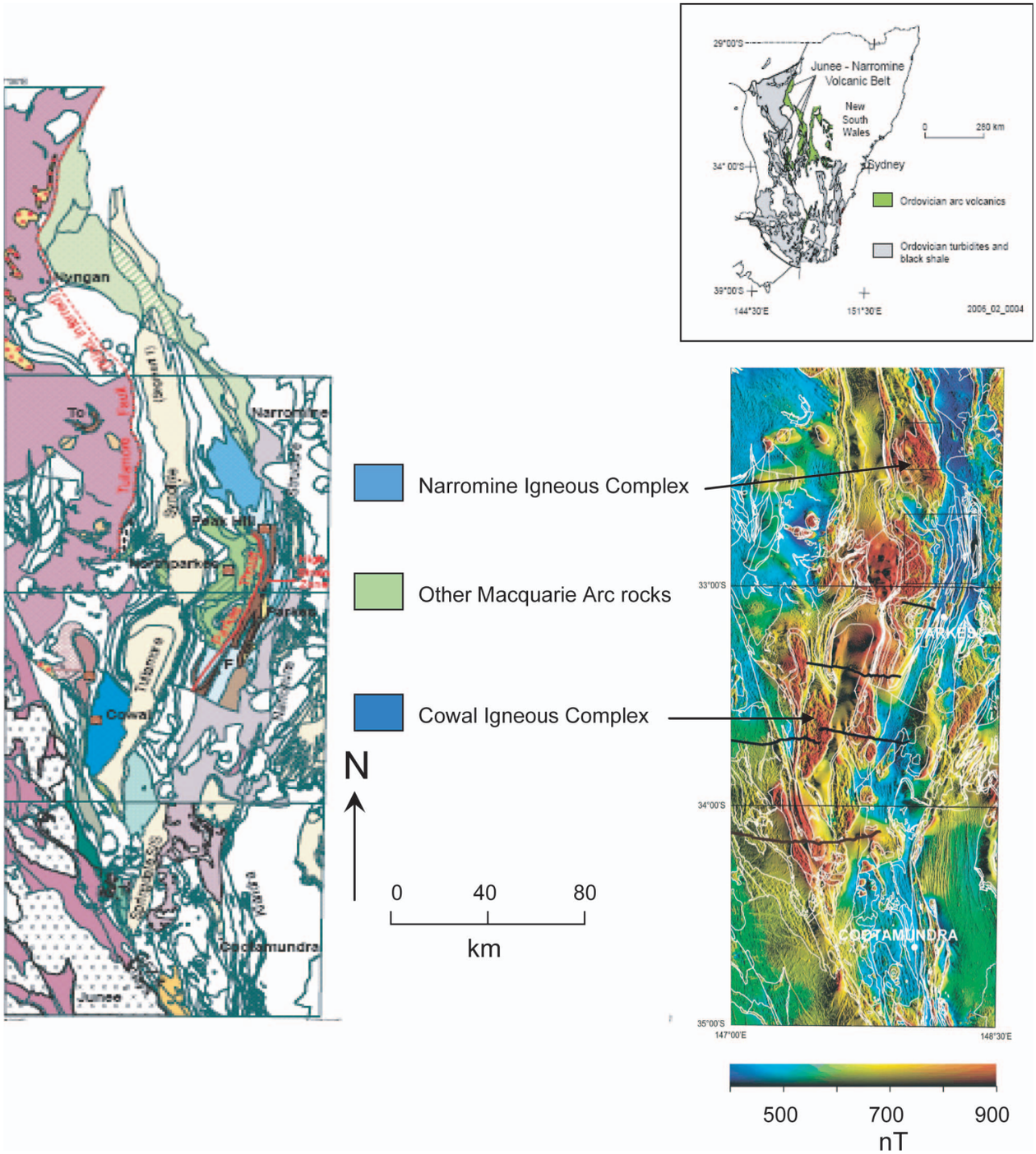

Figure 1 (a) Regional geology map showing key basement units, and (b) regional airborne magnetic map of the Junee–Narromine Volcanic Belt, showing the unexposed Narromine Igneous Complex and Cowal and Fairholme Igneous Complexes. BSZ, Booberoi Shear Zone. Inset map of New South Wales shows the location of the study region.

namely the Narromine, Cowal and Fairholme Igneous Complexes.

NARROMINE IGNEOUS COMPLEX

Outcrop of the Junee–Narromine Volcanic Belt diminishes northwards from Peak Hill towards Narromine (Sherwin 1996), and the magnetically well-defined northern part of this belt occurs entirely in the subsurface (Figure 1). The first major magnetic high in the Junee–Narromine Belt north of Peak Hill marks the 12 × 16 km Narromine Igneous Complex. This complex is buried beneath ~30–100 m of Great Artesian Basin sedimentary rocks.

Around 150 samples were examined in thin-section, and 52 freshest representative samples were analysed for this study of the Narromine Igneous Complex.

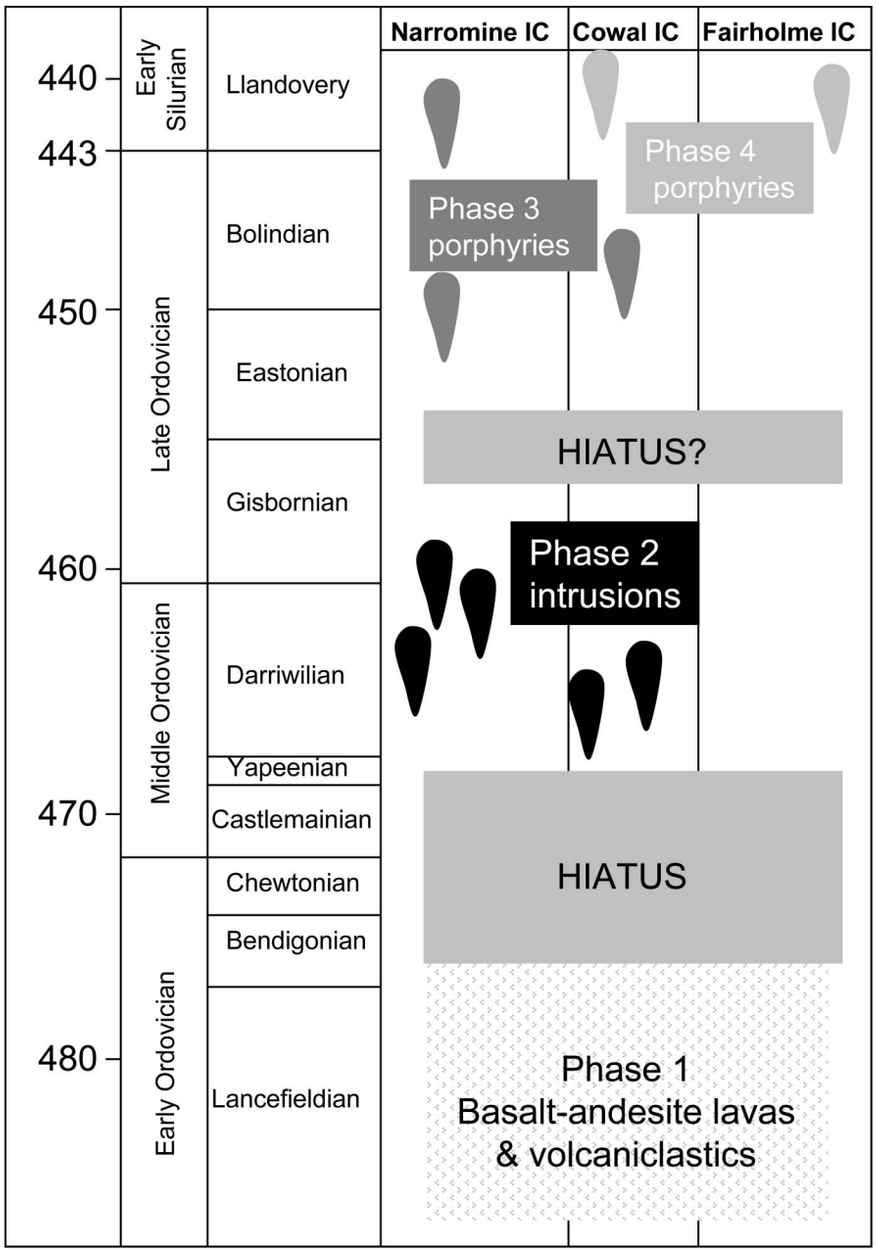

Figure 2 Summary of the lithostratigraphy of the Narromine, Cowal and Fairholme Igneous Complexes showing major magmatic units. The Phase 4 intrusions in the Cowal and Fairholme Igneous Complexes remain undated and are assigned to Phase 4 on their basis of the pronounced shoshonitic compositions.

Samples were sourced from ~150 drillholes (mainly auger core with diamond tails) from a systematic grid-drilling program by Goldfields Exploration and Resolute Ltd aimed at groundtruthing a geophysical interpretation based on gravity and aeromagnetic surveys. Available data show that the Narromine Igneous Complex (Figure 3) consists of probable Ordovician basaltic and andesitic volcanics and volcaniclastic sedimentary rocks that were intruded by large plutons that vary from gabbro or monzogabbro to quartz (monzo)diorite compositions, and a later porphyritic intrusive dacite–granodiorite suite. Interpretation of available gravity and magnetic data (Glen *et al.* 2007d) indicates that the complex is transected by north-northwest-striking major faults (Figure 3). Interpreted Devonian sedimentary rocks border the eastern margin of the Narromine Igneous Complex, whereas Ordovician–Silurian sedimentary rocks occur along its western margins, separated from the Ordovician rocks by a near-vertical fault (Glen *et al.* 2007d). Most studied intrusive rocks were sampled from drillholes between 641500N and 642000N, centred on a major intrusive complex over an across-strike distance of ~15 km in the central part of the magnetic high (Figure 3).

Volcanic and volcaniclastic rocks

Andesitic lavas, lava breccias and volcanic conglomerates are common in the drillholes around the northern margins of the Narromine Igneous Complex, and also along its southwestern margin (Figure 3). In drillhole NACD20, plagioclase phenocryst-rich volcanic sandstones and conglomerates are intruded by dykes and sills of holocrystalline andesite to microdiorite. Most clasts (to several centimetres long) in the conglomerates

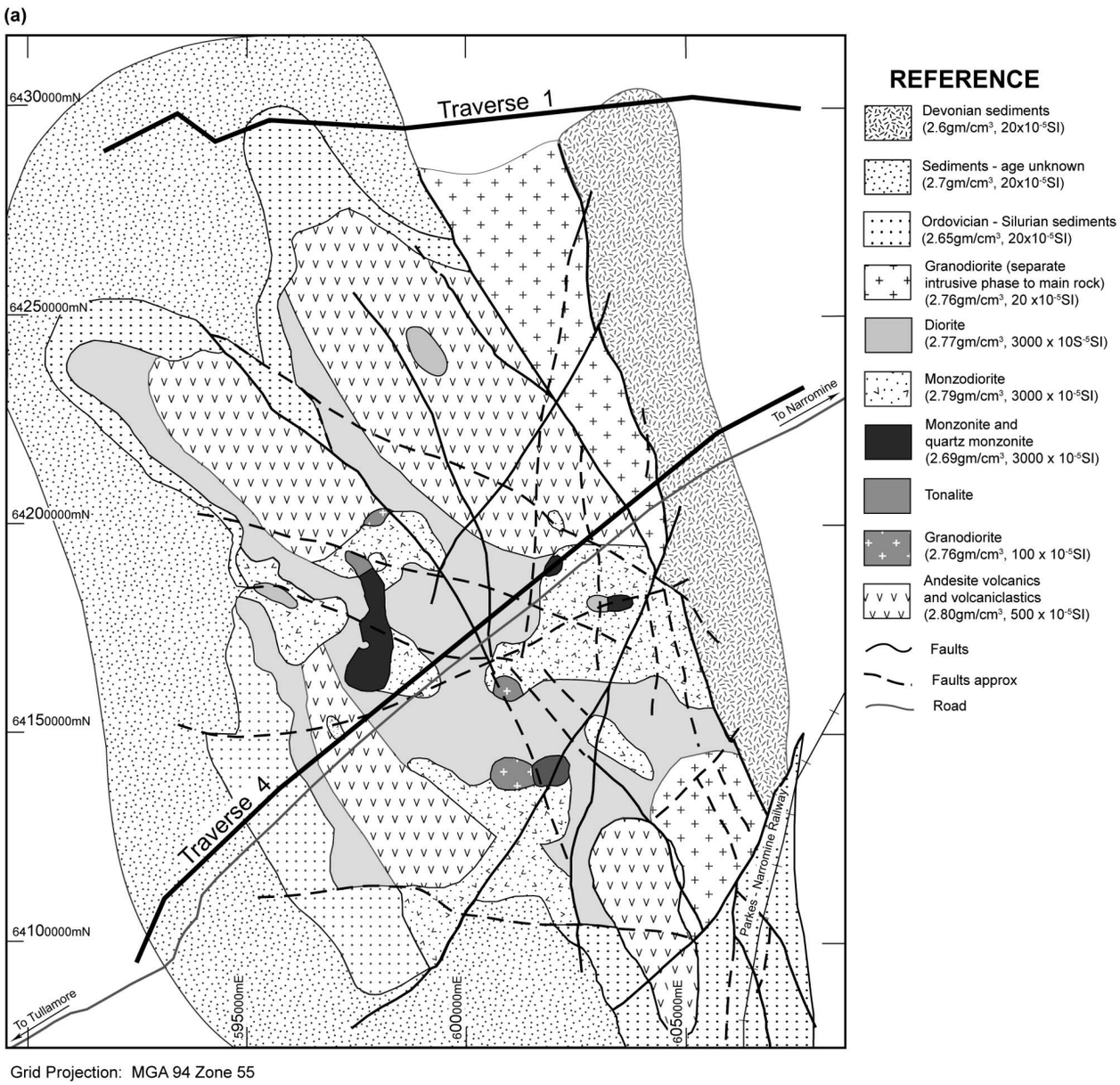

Figure 3 Sketch geological map of the Narromine Igneous Complex (based on data from Goldfields Ltd and Resolute Ltd, and modified after Glen *et al.* 2007d) showing major intrusive units and interpreted extent of Ordovician volcanic and volcaniclastic rocks. Traverse lines 1 and 4 refer to a GS-NSW gravity survey discussed in Glen *et al.* (2007c).

are formerly glassy, sparsely plagioclase-phyric, trachytic-textured lavas. In drillhole NACD137, volcanic clasts and small, medium-grained holocrystalline diorite/monzonitic clasts occur in a conglomerate, attesting to the unroofing and erosion of Early Ordovician(?) intrusive rocks regionally prior to intrusion of the main Narromine Igneous Complex intrusives. Volcanic/volcaniclastic rocks and andesitic/dioritic dykes show mid-greenschist facies assemblages, with abundant epidote.

Andesitic lavas with good textural preservation are present in six drillholes (NACD24, NACD28, NACD31, NACD35, NACD38 and NACD49) and are mainly moderately plagioclase + augite-phyric. In a number of drillholes from the northern part of the complex, limited sample size and quality, and ambiguous textures in thin-section, made it impossible to determine whether some andesites are dykes emplaced at shallow crustal levels, or relatively thick lava flows.

Five samples of Narromine Igneous Complex lavas and dykes were analysed for major and trace elements (Table 1: see Appendix 1 for details of rock types analysed), two of these also for rare-earth elements (REE). Due to the small sample base, we have deliberately restricted this study to determining the affinities of these rocks, and comparing them with better-known suites described from the Parkes – Forbes – Cowal region (Crawford *et al.* 2007).

Apart from one shoshonitic andesite dyke in drillhole NACD105 that has petrographical and geochemical characteristics of the shoshonitic Phase 4 Late

Table 1 Whole-rock compositions (recalculated to 100 volatile-free) of lavas and dykes from the Narromine Igneous Complex.

Sample no.	28-80.0	96-96.0	105-108.4	137-110.0	20-128.9
Easting	601113	601243	601033	598113	596113
Northing	6422184	6412344	6413163	6416734	6420184
SiO_2	63.36	67.93	65.24	47.72	53.31
TiO_2	0.79	1.020.82	0.4	0.86	0.82
Al_2O_3	16.09	17.42	17.37	20.23	18.26
Fe_2O_3	7.71	4.03	4.08	13.45	10.4
MnO	0.12	0.04	0.11	0.79	0.28
MgO	1.25	0.49	1.58	6.43	3.95
CaO	1.45	1.04	3.5	4.18	5.9
Na_2O	4.71	4.51	5.17	5.08	3.73
K_2O	4.71	3.35	2.39	0.96	3.04
P_2O_5	0.35	0.37	0.15	0.28	0.32
LOI	2.2	3.9	2.28	6.42	2.63
Ni	bdl	3	7	16	9
Cr	2	2	19	29	9
V	48	65	80	271	277
Sc	15	19	7	27	22
Zr	329	202	120	56	83
Nb	17.1	9.3	7	3	4.1
Y	40.5	40.4	12	13	15.8
Sr	213	402	855	575	1035
Rb	57	51	32	19	35
Ba	471	557	420	233	682
Pb	5.3	4.8	5.0	6.5	3.1
Zn	131	55	84	1627	164
Cu	171	17	29	41	281
La	34.8	25.1	–	–	14.4
Ce	78.3	55.9	–	–	32.5
Pr	10.68	7.91	–	–	4.54
Nd	44.69	35.92	–	–	20.11
Sm	10.06	8.77	–	–	4.91
Eu	1.94	2.37	–	–	1.57
Gd	8.54	8.96	–	–	4.2
Tb	1.35	1.38	–	–	0.59
Dy	7.72	7.65	–	–	3.18
Ho	1.59	1.53	–	–	0.61
Er	4.52	4.2	–	–	1.71
Yb	4.36	3.73	–	–	1.53
Lu	0.67	0.56	–	–	0.23

bdl, below detection limit.
See Appendix 1 for rock types analysed.

Ordovician Goonumbla and Wombin Volcanics suite (including common apatite microphenocrysts) (Crawford *et al.* 2007), the remainder of the lavas and dykes from the Narromine Igneous Complex are more confidently correlated with the Phase 1 Early Ordovician Nelungaloo Volcanics and correlative lavas in the Cowal Igneous Complex further south (Figure 1). This is consistent with new SHRIMP dates of *ca* 465 Ma (Middle Ordovician) for monzodiorites intruding the volcanic–volcaniclastic package in the Narromine Igneous Complex (see below). A trachyandesite clast from drillhole NACD20, and two probable dykes from NACD28 and NACD96, show strong compositional affinities with the trachyte–trachyandesite suites from the main Cowal mine development at E42 (Golden Lava Unit) and from a drill prospect in the south-central part of the block at E43 (Glen *et al.* 2007b). This is true for both diagnostic trace-element ratios and REE patterns (Figure 4a).

Intrusive rocks

Two petrographically and geochemically distinct intrusive suites are present in the Narromine Igneous Complex. One suite, dominated by monzodiorite, but also including monzogabbros and monzonites, is far more abundant in drillcore. A second suite, composed mainly of rocks varying texturally from porphyritic dacite to holocrystalline granodiorite, occurs as sheet-like sills and dykes intruding the monzodiorite suite rocks, and also as a small pluton ($\sim 2 \times 1$ km) in the central part of the complex.

MONZOGABBRO–MONZODIORITE–MONZONITE SUITE

Abundant medium- to coarse-grained intrusive rocks in the Narromine Igneous Complex range from olivine-bearing monzogabbros, through monzodiorites to subordinate monzonites (the latter present in drillholes NACD2, 77, 81, 85, 87 and 89). All these intrusive rocks show strong mineralogical and textural variation, even over several metres length of drillcore.

The monzogabbros contain occasional altered olivine in drillholes NACD90/136.8 m and 183.9 m, and NACD131/71.8 m, but are dominated by the assemblage Ca-plagioclase–augite–FeTioxides–apatite ± hornblende ± sphene, common interstitial primary brown biotite, and K-feldspar rimming plagioclase. Many show cumulate textures. Primary magmatic hornblende varies from abundant (drillholes NACD118/55.8 m, NACD123/67.1 m, NACD122/65.8 m, NACD125/64.1 m) to minor, and both hornblende and biotite are often replaced by chlorite and epidote, or actinolite in higher-grade rocks. Stout apatite crystals up to almost 1 mm long are common in the monzogabbros, and attest to the early crystallisation of apatite and the shoshonitic nature of the parental magmas to these rocks. With advancing fractionation through monzodioritic to monzonitic compositions, apatite generally decreases in abundance and occurs as more elongate, narrower crystals. Myrmekitic intergrowths are present as interstitial late crystallising material in some monzogabbros (e.g. drillhole NACD131/71.8 m), and interstitial primary quartz becomes an accessory phase in some monzodioritic rocks, although it is rare or absent in the monzonites.

INTRUSIVE DACITE–GRANODIORITE SUITE

A distinctive suite of shallow intrusive porphyritic dacite dykes intrudes the western part of the Narromine Igneous Complex. Intrusive dacites are well represented in drillholes NACD83 (115–150 m), and also occur in NACD82, 87, 89 and 91; in all instances, they intrude quartz-poor monzonitic to monzodioritic host rocks. A single, probably related but intensely silica–sericite–pyrite-altered dacite (not analysed) was encountered in drillhole NACD98 in the eastern part of the intrusive complex, immediately against the eastern boundary fault of the Narromine Igneous Complex. The least-altered dacite sample, from drillhole NACD83/116.6 m, is representative of the suite and is a plagioclase + quartz + hornblende + K-feldspar + FeTioxide + apatite-phyric dacite with fresh hornblende and plagioclase

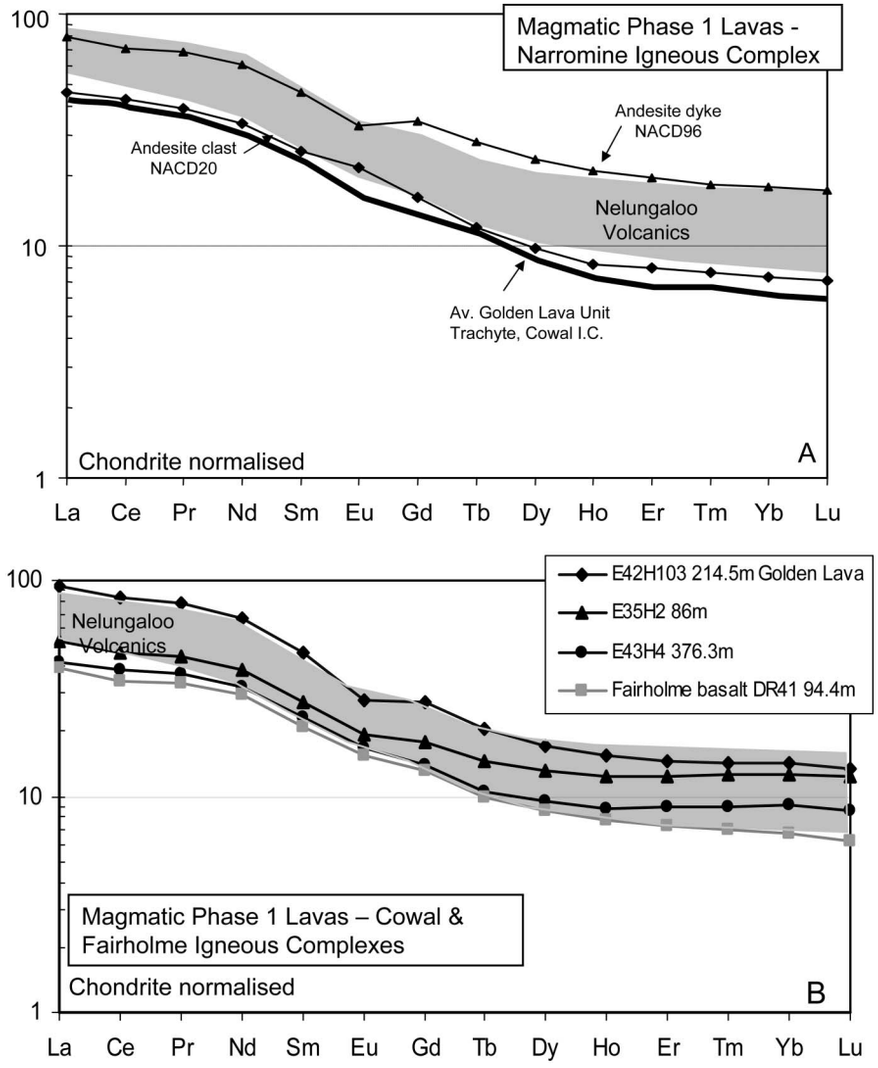

Figure 4 Chondrite-normalised REE patterns for Phase 1 lavas and dykes from the Junee–Narromine Volcanic Belt. (a) Narromine Igneous Complex. (b) Cowal Igneous Complex. In both panels, the field for lavas from the Early Ordovician Nelungaloo Volcanics (Glen *et al.* 2007b) is shown. Normalising values from Boynton (1984).

phenocrysts, and rounded and resorbed quartz phenocrysts in a fine-grained quartzo-feldspathic groundmass. Hornblende phenocrysts are often replaced by chlorite.

Granodiorite occurs mainly in the central western part of Narromine Igneous Complex, as an interpreted $\sim 3.5 \times 1$ km pluton (Figure 3). Granodioritic rocks compositionally identical to the dacite porphyries (see below) consist of blocky abitised plagioclase phenocrysts and occasional smaller hornblende and quartz phenocrysts, set in a groundmass of quartz, albite, K-feldspar and chlorite. The dacites are important, since they are associated with the limited chalcopyrite–pyrite mineralisation, and bear striking petrographic resemblance to host-rocks of the Copper Hill and Cargo mineralisation in the Molong Volcanic Belt. Tourmaline alteration has been noted in drillhole NACD11, associated with sericite–pyrite–carbonate alteration.

Geochronology of Narromine Igneous Complex intrusive rocks

The ages of five samples of Narromine Igneous Complex intrusive rocks have been determined using SHRIMP U–Pb dating of zircons: details of the dating methodology, using the AS3 and SL13 reference zircon standards, are given in Lickfold *et al.* (2007). Three dated samples are from the monzogabbro–monzodiorite–monzonite (MMMz) suite, and two are from the intrusive dacite–granodiorite suite, including one dacite and one granodiorite. Of the former, a hornblende monzodiorite from drillhole NACD125 yielded an age of 461.4 ± 2.6 Ma, a monzonite from drillhole NACD2 yielded an age of 463.3 ± 3.7 Ma, and a monzodiorite from drillhole NACD137 yielded an age of 458.5 ± 4.9 Ma (Table 2; Figure 5a–c). These consistent ages indicate emplacement of the MMMz rocks broadly between 465 and 460 Ma, in mid-Darriwilian times at the end of the Middle Ordovician (following the time-scale in Percival & Glen 2007 figure 2).

Two samples of the intrusive dacite–granodiorite suite from the Narromine Igneous Complex were also dated: a dacite from drillhole NACD83 and a granodiorite from NACD 86. These show almost identical complex age spectra for the analysed grains (Figure 5d, e). Numerous grains have obvious rounded cores interpreted to be inherited zircons. These cores yielded dates

of 467.3 ± 4.8 Ma in the dacite and 470.6 ± 5.5 Ma in the granodiorite, only very slightly older than (and within error of) the dates determined for the Narromine Igneous Complex MMMz suite rocks. However, all zircons studied in both the dacite and the granodiorite have well-developed euhedral outer zones that record ages of 440.9 ± 4.5 Ma in the dacite and 449.4 ± 3.9 Ma in the granodiorite (Table 2; Figure 5d, e). Averaging at 445 Ma (mid-Bolindian, Late Ordovician), these dates agree well within error with available dates for petrographically and compositionally similar intrusive dacites from both Copper Hill and Cargo in the Molong Belt (453–450 Ma) (Crawford *et al.* 2007). A widespread but relatively small volume, medium-K calc-alkaline intrusive event is therefore well documented in the Ordovician belts of central western New South Wales at *ca* 455–445 Ma. We refer to this suite of intrusive dacites and granodiorites as the Copper Hill Suite, after the Copper Hill area near Molong, where rocks of this suite were first thoroughly described (Blevin 2002).

We have no age constraints on the volcanic and volcaniclastic host-rocks to these Darriwilian intrusives in the Narromine Igneous Complex. This 465–460 Ma intrusive event is also well represented in the Cowal Igneous Complex (see below), but the single pre-Late Ordovician intrusive complex dated in the Forbes–Parkes region, the Nelungaloo Intrusives, is significantly older at 481 ± 3 Ma (Butera *et al.* 2001; Simpson *et al.* 2005). In the Molong Belt, Darriwilian rocks comprise the Fairbridge Volcanics, the Cargo Volcanics and possibly the lower Blayney Volcanics, but no contemporaneous holocrystalline intrusive complexes are known from this belt.

Geochemistry of Narromine Igneous Complex intrusive rocks

Representative whole-rock major- and trace-element analyses of 29 least-altered intrusive rocks (excluding narrow dykes) from the Narromine Igneous Complex (seven from the Copper Hill Suite) are given in Table 3 (see Appendix 1 for details of rock types analysed): analytical methods are given in Squire and Crawford (2007). Samples were chosen to cover the geographic and petrographic-compositional range represented among the 125 rocks examined in thin-section.

HOLOCRYSTALLINE MONZOGABBRO–MONZODIORITE–MONZONITE SUITE

The Narromine Igneous Complex holocrystalline intrusive rocks of the MMMz suite define coherent fractionation trends (Figure 6) from relatively low-Mg monzogabbroic rocks to monzodioritic and monzonitic compositions with ~54–62% SiO_2; a single quartz monzonite has 66% SiO_2. The monzogabbros have compositions that trend to lower SiO_2, Fe_2O_3 and TiO_2 (Figure 6) than other rocks in the suite that lack cumulate textures, reflecting accumulation of plagioclase + clinopyroxene + hornblende ± apatite. High P_2O_5 contents in monzogabbros (Table 3) indicate early apatite fractionation, a characteristic of high-K calc-alkaline and shoshonitic lavas. The MMMz suite rocks show mainly high-K calc-alkaline affinities (Figure 6), definitively so for the least-altered rocks; the two monzogabbroic rocks that plot in the low-K field are the most plagioclase + clinopyroxene-rich, hornblende-poor cumulates and are not liquid compositions.

REE patterns for three samples from across the fractionation range of the MMMz suite are shown in Figure 7a. The pattern for a cumulate-textured monzogabbro from drillhole NACD82 reflects the accumulation of plagioclase, clinopyroxene, amphibole and apatite (note positive Eu anomaly), whereas the other two patterns are for rocks that are petrographically more appropriate for near-liquid compositions. Fractionation from monzogabbro with 54% SiO_2 and 3.9% MgO to one with 60% SiO_2 and 2.3% MgO produced a decrease in total REE abundances (Figure 7a), with a steeper drop in MREE than HREE, a feature usually attributable to plagioclase–hornblende–apatite fractionation, and in keeping with the observed phenocryst assemblages. N-MORB normalised multi-element patterns are typical of high-K calc-alkaline and shoshonitic lavas in modern western Pacific arc systems (Figure 7c), and are close to those for plagioclase-phyric lavas from the Walli Volcanics in the Molong Volcanic Belt that also show affinities extending from high-K calc-alkaline to shoshonitic (Crawford *et al.* 2007; Simpson *et al.* 2007). A monzogabbro from NACD97 has an initial ε_{Nd} value of +7.4 calculated at 465 Ma, within the range for the Phase 2 Cargo Volcanics of the same age in the Molong Volcanic Belt (Crawford *et al.* 2007).

COPPER HILL SUITE INTRUSIVE DACITES AND GRANODIORITES

Despite strikingly different textures and grainsize, the porphyritic dacite dykes are compositionally identical to the granodioritic rocks in the western part of the Narromine Igneous Complex, with a relatively restricted SiO_2 range, and together they define coherent and restricted compositional fields on plots against SiO_2 (Figure 6). The dacite–granodiorite compositional fields for many elements and element ratios are clearly separate from those for the MMMz trends. This is especially evident for the K_2O, TiO_2, Zr, Y, Nb and Cr *vs* SiO_2 plots (K_2O, TiO_2, Cr and Zr shown in Figure 6), where the more evolved rocks have consistently lower K_2O, Zr and Nb contents, and notably higher Cr contents than the monzodiorites. No reasonable fractionation scheme can drive the MMMz monzodiorites towards the compositional fields defined by the Copper Hill Suite dacite–granodiorite rocks. Note that a single member of the MMMz suite has 66.7% SiO_2, like the less-evolved dacites, but that this sample has Zr, Y and Nb contents more than twice as high as the intrusive dacite–granodiorite suite rocks at the same SiO_2 level. As indicated by U–Pb SHRIMP zircon dating, the medium-K calc-alkaline Copper Hill Suite dacite–granodiorite intrusions post-date the high-K calc-alkaline to shoshonitic MMMz suite by 15–20 million years.

Table 2 SHRIMP U–Pb zircon results for samples from the Narromine Igneous Complex.

Grain spot	U (ppm)	Th (ppm)	Th/U	$^{206}Pb^*$ (ppm)	$^{204}Pb/^{206}Pb$	f_{206} (%)	Total radiogenic age (Ma)							
							$^{238}U/^{206}Pb$	±	$^{207}Pb/^{206}Pb$	±	$^{206}Pb/^{238}U$	±	$^{206}Pb/^{238}U$	±
NACD 137, 119–120 m (598113E, 6416734N) Age 458.5 ± 5.9 Ma														
1.1	132	66	0.50	8.5	0.000249	0.29	13.380	0.221	0.0586	0.0015	0.0745	0.0013	463.3	7.5
2.1	60	28	0.47	3.7	–	0.78	14.010	0.252	0.0621	0.0022	0.0708	0.0013	441.1	7.8
3.1	149	82	0.55	9.3	0.000591	0.46	13.763	0.190	0.0597	0.0015	0.0723	0.0010	450.1	6.2
4.1	112	52	0.47	7.1	0.000285	0.02	13.652	0.271	0.0563	0.0018	0.0732	0.0015	455.6	8.9
5.1	85	30	0.36	5.5	–	0.16	13.271	0.217	0.0577	0.0017	0.0752	0.0013	467.6	7.6
6.1	97	52	0.53	6.2	–	0.12	13.380	0.217	0.0573	0.0017	0.0746	0.0012	464.1	7.4
7.1	127	47	0.37	8.0	–	0.16	13.618	0.199	0.0574	0.0014	0.0733	0.0011	456.1	6.6
8.1	165	83	0.50	10.5	0.000629	0.12	13.481	0.186	0.0572	0.0012	0.0741	0.0010	460.7	6.3
9.1	154	53	0.34	9.5	–	0.45	13.917	0.189	0.0594	0.0014	0.0715	0.0010	445.4	6.0
10.1	146	57	0.39	9.1	0.000806	−0.04	13.768	0.191	0.0557	0.0014	0.0727	0.0010	452.2	6.2
11.1	149	48	0.32	9.8	–	−0.22	13.164	0.179	0.0547	0.0012	0.0761	0.0011	473.0	6.3
12.1	70	35	0.50	4.6	0.000119	−0.16	12.938	0.211	0.0554	0.0019	0.0774	0.0013	480.7	7.7
13.1	46	16	0.36	2.9	0.000325	0.82	13.373	0.341	0.0629	0.0025	0.0742	0.0019	461.2	11.6
14.1	48	17	0.35	3.0	0.000207	1.52	13.940	0.263	0.0680	0.0026	0.0706	0.0014	440.0	8.3
15.1	216	86	0.40	12.3	0.001045	1.53	15.076	0.196	0.0672	0.0014	0.0653	0.0009	407.9	5.3
16.1	106	44	0.42	6.8	–	1.26	13.366	0.204	0.0664	0.0021	0.0739	0.0012	459.5	7.0
17.1	69	33	0.48	4.5	0.001495	−0.35	13.162	0.236	0.0537	0.0019	0.0762	0.0014	473.6	8.4
18.1	55	16	0.30	3.4	–	0.42	13.915	0.252	0.0592	0.0029	0.0716	0.0013	445.6	8.1
19.1	41	14	0.34	2.7	–	0.06	12.756	0.249	0.0574	0.0024	0.0783	0.0016	486.2	9.4
20.1	43	13	0.30	2.8	0.000628	1.13	13.382	0.254	0.0654	0.0026	0.0739	0.0014	459.5	8.7
NACD 125, 64.1–64.4 m (604613E, 6417684N) Age 461.4 ± 4.2 Ma														
1.1	1191	907	0.76	77.1	–	<0.01	13.270	0.157	0.0561	0.0004	0.0754	0.0009	468.5	5.4
2.1	212	91	0.43	13.7	0.000043	<0.01	13.312	0.167	0.0552	0.0010	0.0752	0.0010	467.6	5.8
3.1	339	144	0.43	21.5	0.000104	0.24	13.560	0.191	0.0581	0.0008	0.0736	0.0011	457.6	6.3
4.1	403	195	0.48	26.7	0.000070	<0.01	12.946	0.149	0.0558	0.0007	0.0773	0.0009	480.1	5.4
5.1	407	217	0.53	25.9	–	<0.01	13.482	0.157	0.0560	0.0007	0.0742	0.0009	461.3	5.3
6.1	173	71	0.41	11.4	0.000286	0.10	13.019	0.169	0.0574	0.0011	0.0767	0.0010	476.6	6.1
7.1	155	57	0.37	9.9	0.000703	0.35	13.450	0.178	0.0591	0.0012	0.0741	0.0010	460.7	6.0
8.1	175	57	0.33	11.0	0.000443	0.46	13.607	0.173	0.0598	0.0011	0.0732	0.0009	455.1	5.7
9.1	286	122	0.43	18.5	–	<0.01	13.243	0.229	0.0543	0.0008	0.0757	0.0013	470.5	8.0
10.1	969	936	0.97	60.7	0.000025	0.04	13.727	0.148	0.0564	0.0004	0.0728	0.0008	453.1	4.8
11.1	298	147	0.49	19.1	–	0.01	13.428	0.157	0.0564	0.0008	0.0745	0.0009	463.0	5.3
12.1	945	690	0.73	59.5	0.000065	<0.01	13.646	0.163	0.0561	0.0006	0.0733	0.0009	455.9	5.3
13.1	307	134	0.44	19.9	0.000030	0.27	13.287	0.156	0.0585	0.0008	0.0751	0.0009	466.6	5.4
14.1	490	269	0.55	30.2	–	0.12	13.943	0.157	0.0568	0.0006	0.0716	0.0008	446.0	4.9
15.1	843	512	0.61	53.1	0.000041	<0.01	13.646	0.147	0.0558	0.0005	0.0733	0.0008	456.1	4.8
16.1	202	83	0.41	12.9	0.000026	0.07	13.478	0.166	0.0568	0.0010	0.0741	0.0009	461.0	5.6
17.1	503	237	0.47	32.8	–	0.02	13.165	0.149	0.0567	0.0006	0.0759	0.0009	471.9	5.2
18.1	443	230	0.52	28.3	0.000067	0.10	13.478	0.154	0.0571	0.0007	0.0741	0.0009	460.9	5.2
19.1	474	229	0.48	30.0	–	0.08	13.581	0.166	0.0568	0.0006	0.0736	0.0009	457.7	5.5
20.1	85	26	0.31	5.4	–	0.22	13.386	0.196	0.0581	0.0015	0.0745	0.0011	463.4	6.7
NACD 2, 82–83 m (603113E, 6418184N) Age 463.3 ± 5.0 Ma														
1.1	266	122	0.46	16.6	0.000667	0.10	13.771	0.174	0.0568	0.0010	0.0725	0.0009	451.4	5.6
2.1	115	44	0.38	7.3	0.000439	0.42	13.553	0.201	0.0595	0.0015	0.0735	0.0011	457.1	6.7
3.1	268	127	0.47	17.6	–	0.03	13.089	0.218	0.0568	0.0010	0.0764	0.0013	474.5	7.8
4.1	335	87	0.26	21.5	0.000082	0.10	13.379	0.163	0.0571	0.0008	0.0747	0.0009	464.2	5.5
5.1	137	39	0.29	8.9	0.000080	0.32	13.149	0.185	0.0591	0.0013	0.0758	0.0011	471.1	6.5
6.1	181	48	0.27	11.8	–	0.01	13.126	0.177	0.0566	0.0012	0.0762	0.0010	473.3	6.3
7.1	410	195	0.48	24.9	–	0.08	14.122	0.174	0.0563	0.0008	0.0708	0.0009	440.7	5.3
8.1	389	171	0.44	22.4	0.000228	0.17	14.928	0.180	0.0565	0.0008	0.0669	0.0008	417.3	5.0
9.1	380	199	0.52	23.3	–	0.31	13.983	0.166	0.0583	0.0008	0.0713	0.0009	443.9	5.2
10.1	222	94	0.42	14.0	0.000083	0.17	13.632	0.162	0.0574	0.0007	0.0732	0.0009	455.6	5.3
11.1	414	182	0.44	26.5	0.000120	0.19	13.387	0.150	0.0578	0.0005	0.0746	0.0009	463.6	5.1
12.1	330	152	0.46	20.6	0.000010	0.09	13.773	0.155	0.0567	0.0006	0.0725	0.0008	451.4	5.0
13.1	229	66	0.29	14.3	0.000198	0.20	13.740	0.162	0.0576	0.0012	0.0726	0.0009	452.0	5.3
14.1	452	196	0.43	29.0	0.000022	0.02	13.399	0.147	0.0564	0.0005	0.0746	0.0008	463.9	5.0
15.1	375	153	0.41	24.1	0.000226	<0.01	13.370	0.149	0.0562	0.0006	0.0748	0.0008	465.0	5.1
16.1	402	189	0.47	26.1	0.000058	0.08	13.242	0.147	0.0571	0.0006	0.0755	0.0009	468.9	5.1
17.1	434	198	0.46	27.8	0.000070	0.01	13.415	0.168	0.0564	0.0005	0.0745	0.0010	463.4	5.7

(*continued*)

Table 2 (*Continued*).

Grain spot	U (ppm)	Th (ppm)	Th/U	$^{206}Pb^*$ (ppm)	$^{204}Pb/^{206}Pb$	f_{206} (%)	Total radiogenic age (Ma)							
							$^{238}U/^{206}Pb$	±	$^{207}Pb/^{206}Pb$	±	$^{206}Pb/^{238}U$	±	$^{206}Pb/^{238}U$	±
18.1	312	126	0.40	20.3	0.000228	<0.01	13.208	0.151	0.0561	0.0006	0.0757	0.0009	470.7	5.3
19.1	291	134	0.46	19.0	0.000000	0.04	13.141	0.148	0.0568	0.0006	0.0761	0.0009	472.6	5.2
4.2	356	166	0.47	22.8	0.000089	<0.01	13.408	0.148	0.0562	0.0006	0.0746	0.0008	463.7	5.0
5.2	191	46	0.24	12.3	0.000277	0.16	13.303	0.161	0.0577	0.0008	0.0750	0.0009	466.5	5.5
NACD 86, 129–130 m (598004E, 6418437N) Age: younger group 449.4 ± 5.0 Ma; older group 470.6 ± 5.5 Ma														
1.1	147	91	0.62	9.1	0.000092	0.32	13.850	0.202	0.0585	0.0014	0.0720	0.0011	448.0	6.4
2.1	43	15	0.36	2.6	0.001923	0.03	14.419	0.323	0.0557	0.0029	0.0693	0.0016	432.1	9.6
2.2	71	29	0.40	4.8	–	0.48	12.736	0.232	0.0607	0.0024	0.0781	0.0015	485.0	8.7
3.1	251	183	0.73	15.4	–	0.29	14.005	0.184	0.0581	0.0010	0.0712	0.0010	443.4	5.7
4.1	48	19	0.39	3.1	–	0.15	13.238	0.270	0.0576	0.0025	0.0754	0.0016	468.8	9.5
5.1	92	43	0.47	5.5	0.000160	0.23	14.269	0.229	0.0574	0.0017	0.0699	0.0011	435.7	6.9
6.1	165	119	0.72	10.1	–	0.25	14.133	0.200	0.0577	0.0014	0.0706	0.0010	439.7	6.1
6.2	90	49	0.55	5.9	0.000536	<0.01	13.151	0.218	0.0557	0.0027	0.0761	0.0013	472.9	7.8
7.1	156	118	0.76	9.3	–	0.17	14.391	0.214	0.0569	0.0014	0.0694	0.0011	432.3	6.3
8.1	50	16	0.31	3.1	0.001303	1.00	14.107	0.277	0.0637	0.0023	0.0702	0.0014	437.2	8.5
9.1	102	46	0.45	6.6	–	0.21	13.360	0.206	0.0580	0.0016	0.0747	0.0012	464.4	7.1
10.1	149	89	0.60	9.5	–	0.16	13.379	0.196	0.0576	0.0014	0.0746	0.0011	464.0	6.7
10.2	105	48	0.46	6.7	–	0.70	13.458	0.184	0.0618	0.0012	0.0738	0.0010	458.9	6.2
11.1	119	72	0.61	7.7	0.000224	0.22	13.198	0.168	0.0582	0.0010	0.0756	0.0010	469.9	5.9
12.1	175	69	0.39	11.2	0.000352	0.28	13.433	0.161	0.0585	0.0009	0.0742	0.0009	461.6	5.4
13.1	89	33	0.37	5.7	0.000106	0.49	13.375	0.223	0.0602	0.0012	0.0744	0.0013	462.6	7.6
14.1	87	43	0.50	5.7	–	0.47	13.122	0.179	0.0603	0.0012	0.0759	0.0011	471.3	6.3
15.1	88	30	0.34	5.8	0.000516	0.58	13.103	0.178	0.0612	0.0012	0.0759	0.0011	471.5	6.3
16.1	183	99	0.54	11.7	0.000321	0.19	13.451	0.185	0.0577	0.0008	0.0742	0.0010	461.5	6.2
17.1	75	23	0.30	4.7	0.000435	1.00	13.792	0.198	0.0640	0.0014	0.0718	0.0010	446.9	6.3
18.1	93	41	0.44	6.1	0.000571	0.47	13.053	0.182	0.0604	0.0012	0.0762	0.0011	473.7	6.5
19.1	45	13	0.29	3.0	0.000887	1.32	13.103	0.213	0.0671	0.0017	0.0753	0.0013	468.0	7.5
20.1	47	14	0.29	3.0	0.000923	1.16	13.704	0.272	0.0653	0.0017	0.0721	0.0015	448.9	8.8
NACD 83, 116 m (598114E, 6417687N) Age: younger group 440.9 ± 5.5 Ma; older group 467.3 ± 4.8 Ma														
1.1	75	34	0.45	4.7	0.000057	0.18	13.758	0.269	0.0574	0.0023	0.0726	0.0015	451.5	8.8
2.1	71	24	0.34	4.2	0.000373	0.19	14.562	0.260	0.0569	0.0022	0.0685	0.0013	427.4	7.6
3.1	91	28	0.31	5.3	0.002959	1.35	14.677	0.234	0.0661	0.0019	0.0672	0.0011	419.3	6.6
4.1	73	28	0.38	4.7	0.000350	0.57	13.319	0.241	0.0609	0.0019	0.0747	0.0014	464.1	8.3
5.1	204	162	0.79	12.9	0.000263	0.40	13.606	0.177	0.0593	0.0011	0.0732	0.0010	455.4	5.8
6.1	237	314	1.32	16.7	0.000202	<0.01	12.186	0.158	0.0566	0.0010	0.0821	0.0011	508.9	6.5
7.1	100	40	0.40	6.2	0.001186	0.39	13.769	0.217	0.0591	0.0016	0.0723	0.0012	450.3	7.0
8.1	538	511	0.95	33.3	–	<0.01	13.888	0.162	0.0552	0.0007	0.0721	0.0009	448.6	5.1
9.1	63	24	0.39	3.9	–	0.39	13.809	0.249	0.0591	0.0021	0.0721	0.0013	449.0	8.0
10.1	56	18	0.32	3.6	0.000602	0.26	13.268	0.233	0.0585	0.0020	0.0752	0.0014	467.2	8.1
11.1	77	38	0.50	5.0	–	0.21	13.161	0.209	0.0582	0.0017	0.0758	0.0012	471.1	7.4
12.1	40	12	0.31	2.6	0.000463	0.75	12.973	0.360	0.0627	0.0025	0.0765	0.0022	475.2	13.0
13.1	126	82	0.65	8.2	–	−0.10	13.193	0.185	0.0557	0.0013	0.0759	0.0011	471.4	6.5
14.1	89	44	0.49	5.8	–	0.36	13.212	0.204	0.0593	0.0016	0.0754	0.0012	468.7	7.1
15.1	120	69	0.57	7.7	0.000740	0.39	13.389	0.199	0.0595	0.0017	0.0744	0.0011	462.6	6.8
16.1	966	973	1.01	25.3	0.006747	13.03	32.790	0.376	0.1534	0.0033	0.0265	0.0003	168.7	2.1
17.1	152	76	0.50	9.3	0.000109	0.37	14.110	0.193	0.0586	0.0012	0.0706	0.0010	439.9	5.9
17.2	271	256	0.95	16.8	–	0.12	13.825	0.168	0.0569	0.0009	0.0723	0.0009	449.7	5.4
18.1	57	17	0.29	3.5	0.000939	0.33	14.072	0.253	0.0584	0.0021	0.0708	0.0013	441.1	7.8
18.2	46	17	0.36	3.1	0.000632	1.70	12.749	0.210	0.0705	0.0018	0.0771	0.0013	478.8	7.8
19.1	45	17	0.38	2.9	0.000751	0.05	13.312	0.239	0.0568	0.0021	0.0751	0.0014	466.7	8.3
19.2	75	42	0.56	4.7	0.000590	0.73	13.628	0.195	0.0619	0.0013	0.0728	0.0011	453.3	6.4
20.1	117	57	0.49	7.8	0.000374	0.38	12.889	0.167	0.0598	0.0012	0.0773	0.0010	480.0	6.1
21.1	104	66	0.63	6.2	0.000338	1.52	14.568	0.191	0.0675	0.0016	0.0676	0.0009	421.7	5.5
22.1	174	134	0.77	10.5	0.000258	0.80	14.286	0.186	0.0619	0.0010	0.0694	0.0009	432.8	5.5
23.1	207	132	0.64	13.5	0.000091	0.27	13.200	0.155	0.0586	0.0009	0.0756	0.0009	469.5	5.4
24.1	141	82	0.58	8.8	0.000219	0.67	13.643	0.171	0.0615	0.0010	0.0728	0.0009	453.0	5.6

Uncertainties given at the 1σ level. Error in AS3 reference zircon calibration was 0.35 and 0.62%% for the analytical sessions (not included in above errors but required when comparing data from different mounts). f_{206} % denotes the percentage of ^{206}Pb that is common Pb. Correction for common Pb made using the measured $^{238}U/^{206}Pb$ and $^{207}Pb/^{206}Pb$ ratios following Tera and Wasserburg (1972) as outlined in Williams (1998).

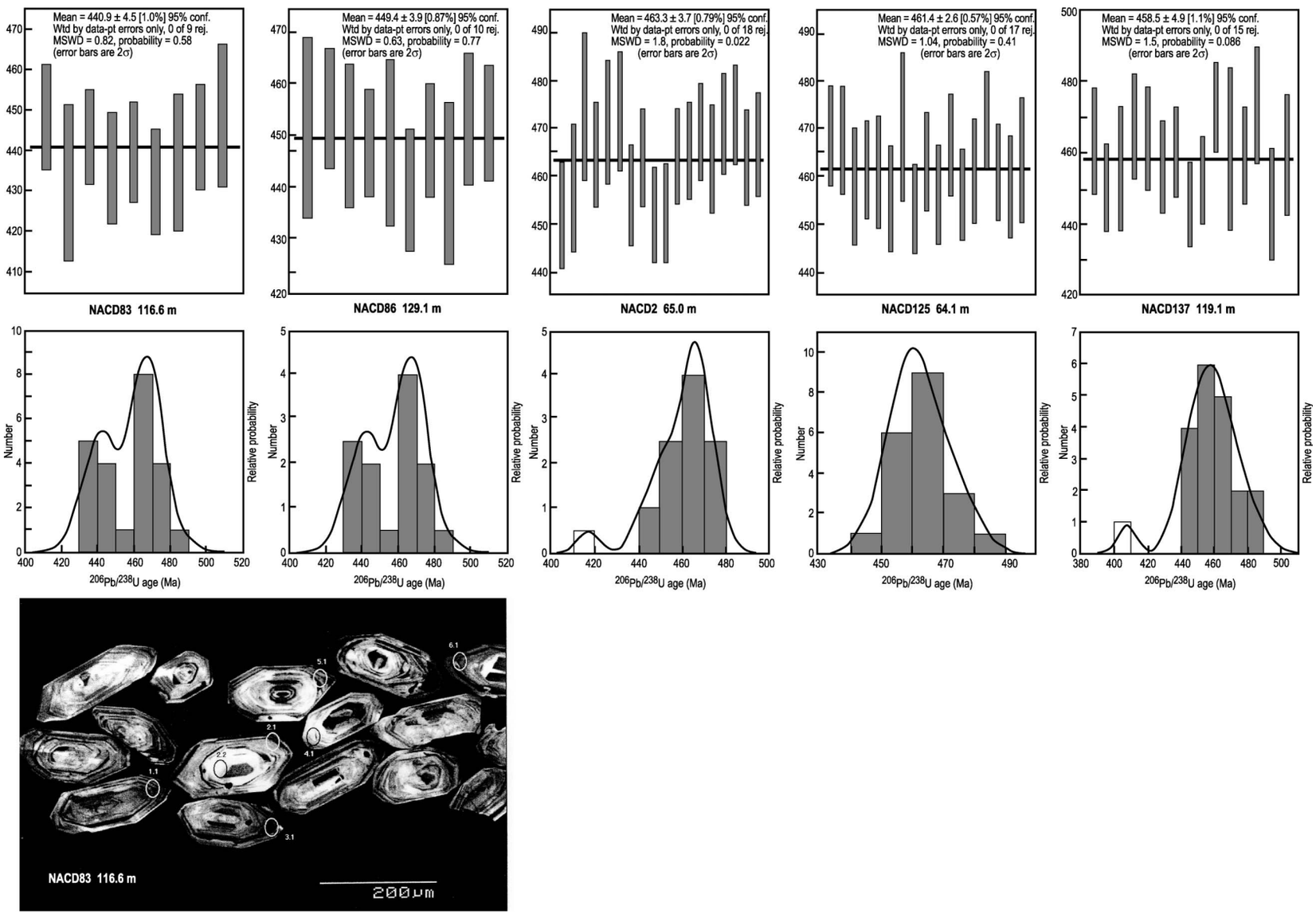

Figure 5 U–Pb in zircon SHRIMP ages for two monzodiorites (NACD125, NACD137) and a monzonite (NACD2) from the MMMz suite, and a granodiorite (NACD86) and a porphyritic intrusive dacite (NACD83) from the Copper Hill Suite, all from the Narromine Igneous Complex, showing (Top) weighted mean age calculations of the $^{206}Pb/^{238}U$ age, and (Middle) relative probability plot with stacked histogram of the $^{206}Pb/^{238}U$ ages. (Bottom) Cathodoluminescene image of some zircons in NACD83 116.6 m showing spots dated by SHRIMP, and rounded and resorbed magmatic cores overgrown by zoned rims. See Table 2 for GDA coordinates of samples.

A number of compositional features of the Copper Hill Suite invite comparison with Cenozoic adakites. These include the absence of compositions more mafic than 67% SiO_2 and the strikingly high Sr/Y values for such felsic magmas (80–95: Table 3). However, a characteristic feature of adakitic dacites is their notable HREE depletion (Defant & Drummond 1990), and this feature is not shared by the Copper Hill Suite rocks (Figure 7b), including those in the Narromine Igneous Complex, and elsewhere in the disrupted Macquarie Arc. The high Sr–low Y characteristics of the Copper Hill Suite rocks in the Narromine Igneous Complex are more reasonably accounted for by significant apatite–hornblende fractionation from parental magmas with very high Sr contents.

A dacite and a granodiorite from the Narromine Igneous Complex Copper Hill Suite have initial ε_{Nd} values of +6.4 and +6.9, respectively (Crawford *et al.* 2007), little different from that of depleted mantle at 445 Ma, indicating minimal involvement of any component derived from ancient continental crust in the genesis of this suite. Further discussion of the petrogenesis of the Copper Hill Suite follows presentation of data for intrusive rocks in the Cowal Igneous Complex.

Table 3 Whole-rock major- and trace-element data (recalculated to 100% volatile-free) for Narromine Igneous Complex intrusive holocrystalline rocks of the Monzogabbro–Monzodiorite–Monzonite Suite, and intrusive dacite porphyries and granodiorites of the Copper Hill Suite.

Sample no.	68-101.4	82-143.8	85-132.7	89-197.0	90-144.0	90-183.8	92-61.2	129-134	105-103.4	2-65.0	96-102.6
Suite	Monzogabbro–Monzodiorite–Monzonite Suite										
Easting	597873	598617	598362	597613	597853	597853	595713	597113	601033	603113	601113
Northing	6414060	6418184	6418167	6419184	6417184	6417184	6418484	6419184	6413163	6418184	6412184
SiO_2	58.17	51.03	66.52	59.23	49.33	50.60	49.62	55.32	60.37	58.62	61.53
TiO_2	0.79	1.02	0.53	0.72	0.65	0.74	0.78	0.90	0.88	0.71	0.52
Al_2O_3	15.92	18.37	15.11	19.28	19.43	17.31	18.72	17.29	17.80	19.24	18.08
Fe_2O_3	9.03	11.34	5.00	7.17	9.96	10.66	10.13	9.43	7.55	6.32	6.12
MnO	0.10	0.30	0.29	0.20	0.17	0.18	0.40	0.27	0.19	0.08	0.22
MgO	3.00	4.38	1.99	4.80	6.10	6.69	6.60	3.77	2.30	1.78	2.47
CaO	4.82	7.10	5.62	2.83	10.74	9.88	9.50	7.52	2.89	4.56	3.21
Na_2O	5.62	4.47	3.14	3.18	3.05	3.30	2.94	3.27	4.81	5.12	6.82
K_2O	2.09	1.45	1.67	2.33	0.43	0.42	1.04	1.83	2.77	3.30	0.82
P_2O_5	0.45	0.54	0.14	0.26	0.15	0.21	0.27	0.40	0.45	0.28	0.21
LOI	1.88	2.33	4.34	4.32	1.51	1.50	2.63	1.88	3.75	1.65	2.29
Ni	3	7	4	7	32	34	18	8	2	3	7
Cr	3	13	7	8	66	69	88	8	2	3	7
V	134	333	91	204	263	319	256	219	122	136	145
Sc	22	24	9	16	25	25	31	20	19	13	9
Zr	163	47	212	117	19	35	52	152	171	141	93
Nb	*8.3*	*2.5*	*12.1*	*6.8*	2	3	3	9	*7.1*	8	*5.3*
Y	34	15	22	20	9	11	17	25	26	21	12
Sr	524	1053	539	755	1121	912	716	862	842	918	713
Rb	18	22	29	41	4	4	23	25	43	50	9
Ba	386	339	186	323	121	154	82	284	705	373	144
Pb	*2.1*	*3.4*	*3.8*	*4.8*	1.6	2.3	3.7	5.4	5.8	4.7	*22.6*
Zn	55	135	148	158	108	83	168	179	131	66	171
Cu	14	284	5	309	85	95	65	215	87	335	28
La	*18.51*	*13.20*	*19.94*	*14.24*	–	–	–	–	*13.12*	–	*10.71*
Ce	*39.52*	*29.30*	*40.22*	*30.33*	–	–	–	–	*25.61*	–	*22.10*
Pr	*5.23*	*4.25*	*5.08*	*4.08*	–	–	–	–	*3.14*	–	*2.89*
Nd	*22.77*	*19.77*	*20.51*	*17.7*	–	–	–	–	*12.46*	–	*12.24*
Sm	*6.02*	*4.95*	*4.44*	*4.22*	–	–	–	–	*2.71*	–	*2.87*
Eu	*1.60*	*1.95*	*1.21*	*1.57*	–	–	–	–	*0.82*	–	*0.95*
Gd	*6.23*	*4.37*	*4.07*	*4.18*	–	–	–	–	*2.30*	–	*2.63*
Tb	*1.04*	*0.59*	*0.65*	*0.64*	–	–	–	–	*0.36*	–	*0.41*
Dy	*6.18*	*3.05*	*3.71*	*3.7*	–	–	–	–	*2.03*	–	*2.24*
Ho	*1.29*	*0.58*	*0.77*	*0.76*	–	–	–	–	*0.41*	–	*0.46*
Er	*3.65*	*1.46*	*2.27*	*2.14*	–	–	–	–	*1.23*	–	*1.31*
Yb	*3.34*	*1.18*	*2.36*	*1.97*	–	–	–	–	*1.22*	–	*1.23*
Lu	*0.51*	*0.18*	*0.37*	*0.3*	–	–	–	–	*0.18*	–	*0.19*
Hf	*4.26*	*1.30*	*4.97*	*2.71*	–	–	–	–	*3.14*	–	*2.33*
Ta	*0.45*	*0.14*	*0.81*	*0.43*	–	–	–	–	*0.48*	–	*0.33*
Th	*2.99*	*0.99*	*3.75*	*1.60*	–	–	–	–	*2.14*	–	*1.35*
U	*1.20*	*0.49*	*1.83*	*0.96*	–	–	–	–	*1.06*	–	*0.62*

(*continued*)

Table 3 (*Continued*).

Sample no.	97-53.0	118-55.8	119-35.7	119-58.9	121-80.7	122-65.8	125-64.1	126-60.0	130-86.9	131-79.8	135-97.4
Suite	Monzogabbro – Monzodiorite – Monzonite Suite										
Easting	604113	603613	603613	603613	604113	604613	604613	603113	603613	604113	602613
Northing	6417184	6418184	6417734	6417734	6417684	6417184	6417684	6417684	6418684	6418684	6418684
SiO_2	54.03	55.67	50.37	51.24	58.32	56.04	57.00	54.43	55.04	56.02	59.32
TiO_2	0.91	0.75	0.93	1.00	0.58	0.89	0.63	0.82	0.83	0.71	0.64
Al_2O_3	17.79	18.55	17.49	17.44	18.63	17.78	19.91	18.60	18.16	18.00	19.21
Fe_2O_3	9.24	7.47	10.83	11.02	6.73	8.40	6.18	8.59	8.65	7.94	5.24
MnO	0.20	0.18	0.22	0.20	0.15	0.18	0.14	0.17	0.21	0.17	0.15
MgO	3.90	2.61	4.92	4.75	3.25	3.08	2.45	3.31	3.76	3.12	2.06
CaO	6.99	8.12	8.19	9.15	5.36	6.26	5.09	7.16	5.16	6.29	3.90
Na_2O	4.38	4.74	4.25	3.77	5.05	4.63	5.76	4.67	5.32	4.99	6.53
K_2O	2.04	1.57	1.97	1.11	1.69	2.26	2.46	1.77	2.47	2.46	2.63
P_2O_5	0.52	0.35	0.84	0.33	0.24	0.47	0.37	0.47	0.40	0.30	0.32
LOI	1.79	2.12	2.48	1.36	2.74	1.51	2.17	2.00	2.90	1.83	3.50
Ni	6	4	7	8	9	6	2	6	4	3	2
Cr	11	5	8	8	22	10	4	14	5	4	2
V	269	198	365	402	165	218	154	285	258	218	120
Sc	18	16	21	25	10	18	12	20	18	17	12
Zr	149	107	75	83	96	71	127	90	110	123	164
Nb	*5.8*	6	4	4	6	7	6.0	4.7	5	6	7
Y	19	18	17	15	12	20	16	18	18	17	17
Sr	1132	1101	1115	1094	933	855	1009	1032	908	881	555
Rb	33	20	32	14	27	31	37	21	37	36	36
Ba	675	209	257	208	339	316	417	329	395	309	313
Pb	*5.8*	6.2	2.2	2.7	1.8	3.9	*3.8*	*4.7*	2.6	2.7	3.3
Zn	108	79	104	99	99	91	72	104	87	93	80
Cu	337	118	559	587	113	332	96	268	215	111	114
La	*19.30*	–	–	–	–	–	*20.05*	*18.40*	–	–	–
Ce	*42.31*	–	–	–	–	–	*43.32*	*39.74*	–	–	–
Pr	*5.89*	–	–	–	–	–	*5.9*	*5.43*	–	–	–
Nd	*25.8*	–	–	–	–	–	*24.84*	*23.72*	–	–	–
Sm	*5.89*	–	–	–	–	–	*5.81*	*5.36*	–	–	–
Eu	*1.76*	–	–	–	–	–	*1.75*	*1.69*	–	–	–
Gd	*5.05*	–	–	–	–	–	*4.77*	*4.56*	–	–	–
Tb	*0.71*	–	–	–	–	–	*0.67*	*0.64*	–	–	–
Dy	*3.71*	–	–	–	–	–	*3.53*	*3.42*	–	–	–
Ho	*0.71*	–	–	–	–	–	*0.68*	*0.65*	–	–	–
Er	*1.89*	–	–	–	–	–	*1.86*	*1.77*	–	–	–
Yb	*1.66*	–	–	–	–	–	*1.64*	*1.58*	–	–	–
Lu	*0.24*	–	–	–	–	–	*0.24*	*0.23*	–	–	–
Hf	*2.68*	–	–	–	–	–	*2.58*	*2.49*	–	–	–
Ta	*0.34*	–	–	–	–	–	*0.22*	*0.25*	–	–	–
Th	*2.56*	–	–	–	–	–	*1.84*	*2.02*	–	–	–
U	*1.28*	–	–	–	–	–	*0.87*	*0.77*	–	–	–

(*continued*)

Alteration of the Narromine Igneous Complex Copper Hill Suite dacites and granodiorites

Weakly developed Cu – Au mineralisation occurs in the central section of the western Narromine Igneous Complex (Cooke *et al.* 2007). Mineralisation is spatially (and genetically?) associated with the intrusive dacites – granodiorites of the Copper Hill Suite, which has intruded the MMMz suite rocks, also shown in drillholes NACD 8, 83, 89 and 91. A propylitic alteration assemblage (epidote – chlorite – carbonate – quartz – sericite) is developed in the dacitic and granodioritic rocks. Cu – (Au) mineralisation occurs primarily as quartz-magnetite – epidote – chlorite – chalcopyrite veins, and also as minor disseminations in propylitic-altered rocks. The dacites have also undergone localised intense sericite – carbonate – pyrite – (chlorite) alteration near major faults. However, this hydrothermal activity is not associated with any known mineralisation. Significant hydrothermal alteration is indicated by occasional adularia veinlets in drillhole NACD68 (at 98.5 m).

Calculated temperatures of formation for the propylitic alteration assemblage and related quartz – epidote – magnetite – chalcopyrite veins are between 350 and 450°C, based on O-isotope results and application of the quartz – epidote geothermometer. Hypersaline fluid inclusions have been observed locally in quartz phenocrysts and quartz – epidote veins, indicating the presence of magmatic – hydrothermal fluids typical of porphyry-style mineralisation. Apart from the local intensive development of 'epidosite', and the aforementioned barren sericitic alteration, alteration

Table 3 (*Continued*).

Sample no.	82-120.0	83-116.6	83-148.4	89-137.2	8-137.7	86-129.1	137-119.1
Suite				Copper Hill Suite			
Easting	598617	598114	598114	597613	598027	598004	598113
Northing	6418184	6417687	6417687	6419184	6418273	6418437	6416734
SiO_2	70.01	67.58	68.53	69.99	69.39	68.05	66.67
TiO_2	0.26	0.26	0.26	0.30	0.26	0.29	0.31
Al_2O_3	16.14	15.81	16.28	16.72	15.95	16.50	17.20
$Fe2O_3$	3.04	5.30	3.55	2.75	3.31	4.29	4.32
MnO	0.09	0.04	0.08	0.04	0.11	0.06	0.23
MgO	1.29	1.09	1.14	2.02	1.33	1.38	1.69
CaO	1.68	2.85	2.74	1.55	1.79	2.68	1.89
Na_2O	5.28	4.77	5.10	4.97	4.51	4.54	5.22
K_2O	2.12	2.18	2.23	1.56	3.28	2.10	2.37
$P2O_5$	0.09	0.11	0.09	0.09	0.09	0.11	0.10
LOI	2.16	0.97	1.79	2.84	1.79	1.61	2.01
Ni	5	5	7	bdl	9	7	7
Cr	22	20	23	22	24	25	31
V	55	54	57	86	52	57	68
Sc	4	5	5	7	4	5	4
Zr	98	103	97	102	98	97	100
Nb	5	6	*5.7*	*6.5*	*6.7*	*6.0*	*5.9*
Y	8	8	8	9	7	8	7
Sr	593	718	659	728	571	762	541
Rb	26	23	27	0	43	22	37
Ba	524	447	511	207	650	480	538
Pb	8.8	4.8	*7.0*	*1.8*	*4.6*	*4.3*	*4.8*
Zn	71	44	51	0	100	80	193
Cu	249	408	96	0	1542	73	15
La	–	–	*10.33*	*16.62*	*12.20*	*9.52*	*8.30*
Ce	–	–	*18.24*	*30.94*	*21.41*	*17.30*	*15.83*
Pr	–	–	*2.08*	*3.67*	*2.27*	*1.98*	*1.88*
Nd	–	–	*7.97*	*14.33*	*7.91*	*7.33*	*7.34*
Sm	–	–	*1.63*	*2.80*	*1.42*	*1.51*	*1.50*
Eu	–	–	*0.57*	*1.22*	*0.39*	*0.52*	*0.48*
Gd	–	–	*1.39*	*2.41*	*1.20*	*1.30*	*1.25*
Tb	–	–	*0.22*	*0.34*	*0.18*	*0.21*	*0.19*
Dy	–	–	*1.25*	*1.98*	*1.04*	*1.2*	*1.14*
Ho	–	–	*0.26*	*0.41*	*0.22*	*0.26*	*0.24*
Er	–	–	*0.78*	*1.18*	*0.70*	*0.76*	*0.76*
Yb	–	–	*0.85*	*1.13*	*0.81*	*0.88*	*0.81*
Lu	–	–	*0.14*	*0.17*	*0.14*	*0.15*	*0.13*
Hf	–	–	*2.44*	*2.48*	*2.52*	*2.59*	*2.32*
Ta	–	–	*0.39*	*0.43*	*0.56*	*0.45*	*0.42*
Th	–	–	*1.76*	*1.90*	*2.68*	*1.93*	*1.17*
U	–	–	*1.27*	*1.05*	*3.03*	*0.81*	*0.57*

Trace elements in italics measured by ICP-MS, remainder and majors by XRF. bdl, below detection limit. See Appendix 1 for rock types analysed.

assemblages intersected during drilling of the Narromine Igneous Complex are only weakly developed, indicating low fluid fluxes and limited mineral potential. Magnetite-destructive alteration zones appear not to be prospective for copper–gold mineralisation, based on the material intersected to date.

COWAL AND FAIRHOLME IGNEOUS COMPLEXES

South of Forbes, the Junee–Narromine Volcanic Belt is defined by a number of unexposed but aeromagnetically defined bodies, including the Cowal Igneous Complex east of the Booberoi Shear Zone and the Fairholme Igneous Complex west of the fault (Figure 8). North Ltd, and more recently Barrick Gold Ltd, carried out extensive exploration in the Cowal Igneous Complex (Miles & Brooker 1998; Bywater *et al.* 2004) with widespread aircore programs that in many instances have yielded good rock samples from diamond tails. Specific target areas recognised as Endeavour (E)35, E39, E41, E42 and E43 cover a large part of the central and western part of the Cowal Igneous Complex (Figure 8), and a few diamond drillholes in the northern part (LCD12, LCD13) provided further material for study. E42 is in development to be a significant gold mine with an estimated resource of 63.6 Mt @ 1.22 g/t

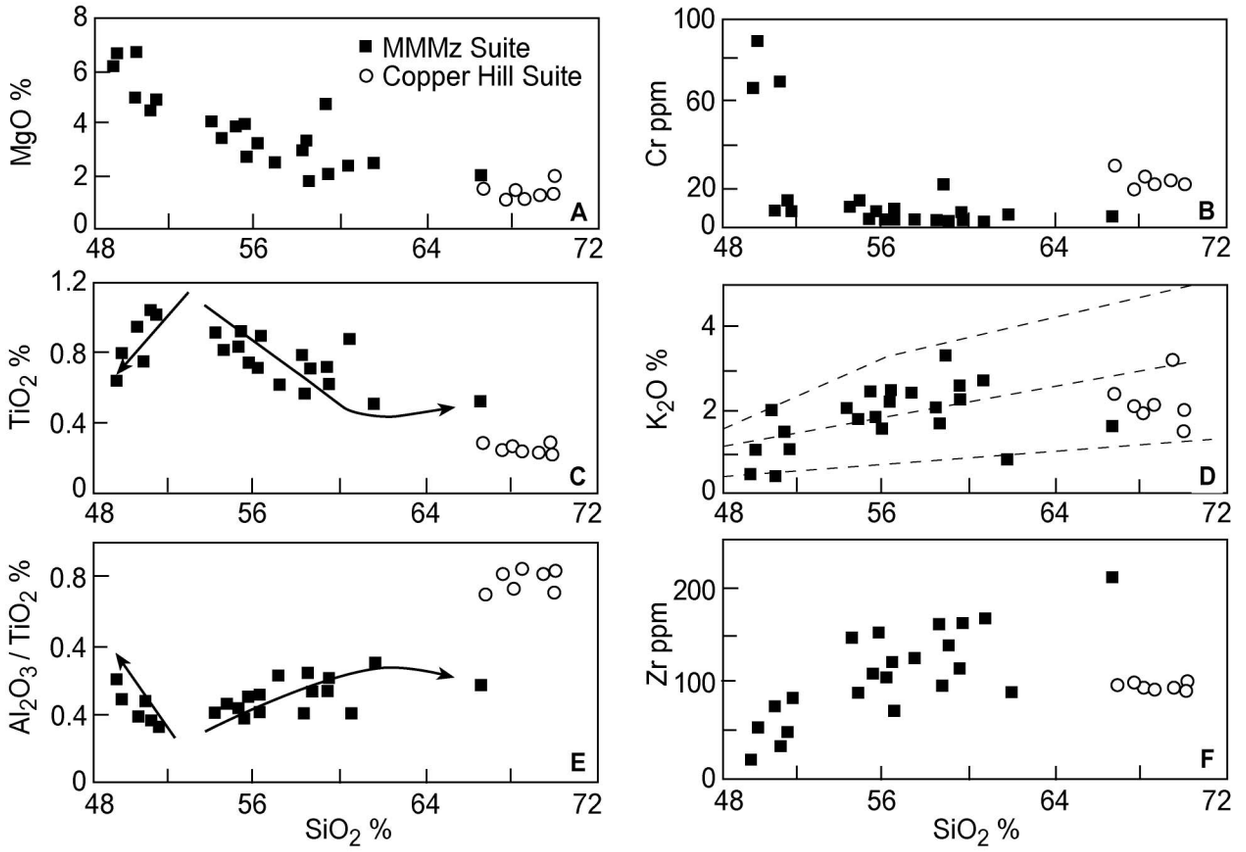

Figure 6 Some major and trace elements *vs* SiO_2 for intrusive rocks from the Narromine Igneous Complex, chosen to show distinct compositional fields for the MMMz suite compared to the granodioritic and dacitic–rhyolitic rocks assigned to the Phase 3 Copper Hill Suite. Arrows in the MMMz suite show trends for accumulation of a plagioclase–clinopyroxene–hornblende-dominant assemblage (<52% SiO_2) and an interpreted liquid line of descent (>52% SiO_2).

gold (Bywater *et al.* 2004). Newcrest's Marsden prospect, close to the southeastern faulted margin of the Cowal Igneous Complex (Figure 8), has been the subject of ongoing exploration, and Newcrest also carried out drilling at several prospects in the Fairholme Igneous Complex.

Cowal Igneous Complex

Due to complete burial by much younger cover, including the Quaternary sediments of Lake Cowal, the only part of the Cowal Igneous Complex in which a lithostratigraphy (albeit of limited extent and thickness) has been determined is around E42 (the Cowal gold deposit), where a sequence of trachytic lavas and volcaniclastics has been recognised (Miles & Brooker 1998). These rocks, including the main volcanic unit, the Golden Lava, have been intruded by a major dioritic intrusion, the Muddy Lake Gabbro, for which available radiometric dates suggest a Middle Ordovician age (465–456 Ma: see below). Interpretation of aeromagnetic data (Figure 1) by exploration groups, groundtruthed by aircore sampling, suggests that much of the southern Cowal Igneous Complex may be made up of Ordovician intrusive rocks, with at least one high-level granodioritic intrusion known from drillholes LCD12 and 13 in the northern part of the complex. Eastonian limestone is known from the Marsden area, but its relationships with the adjacent rocks remain unknown (Percival & Glen 2007).

VOLCANIC AND VOLCANICLASTIC ROCKS

Away from E42, lavas are poorly represented in the Cowal Igneous Complex. Two analyses of lavas, one andesitic, the other basaltic, from E46 (Figure 8), were reported by Bastrakov (1998). Lavas are also present in drillholes around E43, most being of trachyandesite to trachyte compositions with phenocrysts of plagioclase, augite, FeTi oxides and apatite microphenocrysts. Formerly glassy textures are common. Four lavas from the E43 prospect west of Marsden have been analysed (Table 4: see Appendix 1 for details of rock types analysed), and these range from 55 to 67% SiO_2.

Lavas are well represented from the E42 area drilling, with nine samples of the Golden Lava trachyandesites–trachytes chosen for whole-rock analysis (Table 4). These lavas are all formerly glassy, often spherulitic or banded felsic lavas with sparse plagioclase phenocrysts, rare chloritised mafic phenocrysts, and common apatite microphenocrysts. They are best classified as trachyandesites to trachytes, with 61–67% SiO_2, a range probably exaggerated by SiO_2 mobility

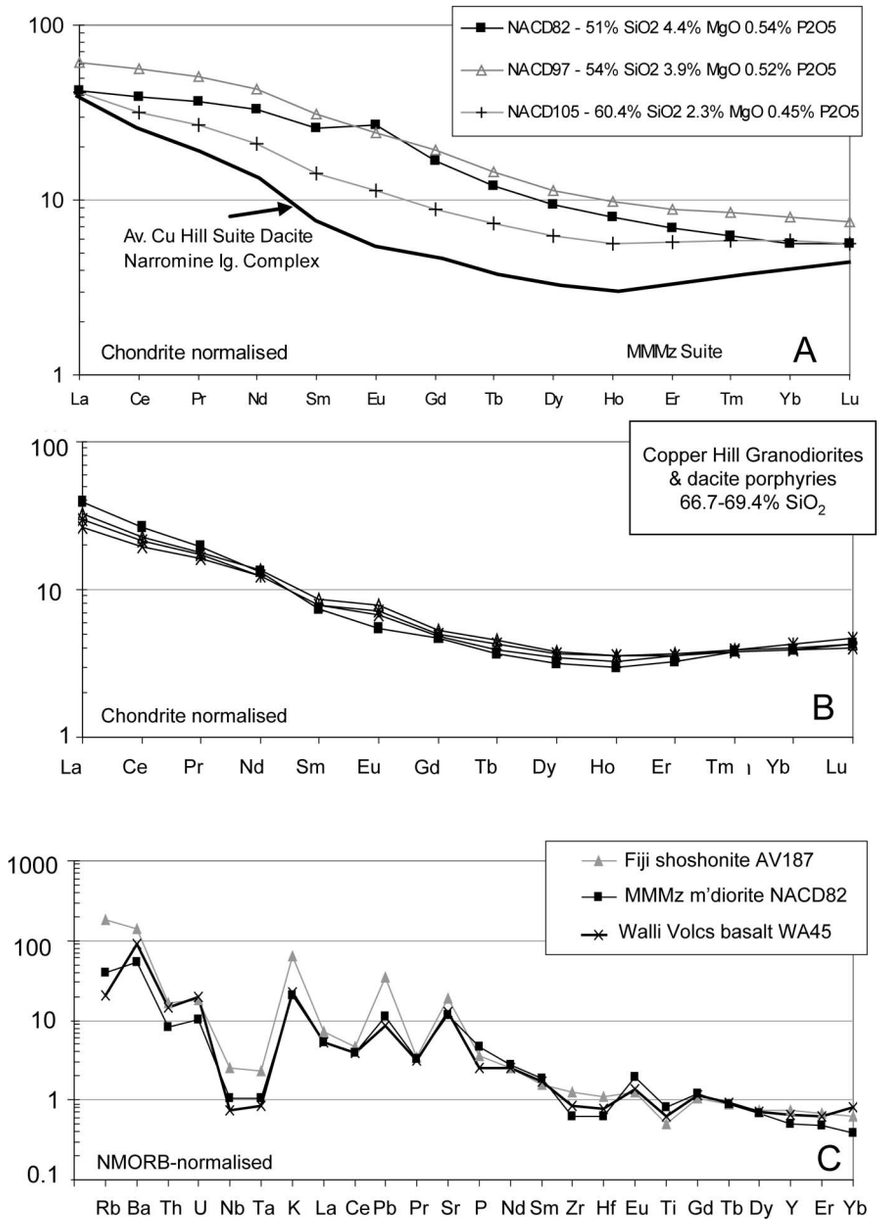

Figure 7 Chondrite-normalised REE patterns for (a) a monzogabbro and two monzodiorites from the MMMz suite, and (b) granodiorites and intrusive dacite porphyries from the Copper Hill Suite, both from the Narromine Igneous Complex. (c) N-MORB normalised multi-element patterns for an average MMMz suite monzodiorite compared with a typical Fijian shoshonite lava and an average Walli Volcanics basalt from the Molong Volcanic Belt (standardising data from Sun & McDonough 1989; data from Crawford *et al.* 2007).

during alteration. The single more mafic rock from E42 classified petrographically as a lava (E42H361-340.6) is a plagioclase+augite-phyric trachyandesite with 52% SiO_2 and 5.5% MgO, and a REE pattern (Figure 4b) perfectly parallel to those for the felsic lavas, suggesting that is a more mafic comagmatic representative of the same suite (see below).

Geochemical affinities of the Phase 1 Golden Lava trachytes and trachyandesites and associated feeder dykes from E42 have been described in Glen *et al.* (2007a). At 62–65% SiO_2, best-preserved lavas have 3.5–4.5% K_2O and 0.40–0.45% P_2O_5, falling in the high-K calc-alkaline series close to the border with shoshonitic lavas (Figure 6d). The E42 lavas were therefore considered to be more fractionated variants of the same broad high-K calc-alkaline magma type as the Phase 1 Nelungaloo Volcanics west of Parkes, some 50 km northeast of Cowal.

Only four lavas are recorded by drilling at E43 and E46, and these vary from trachyandesitic to trachytic compositions. An REE pattern (Figure 4b) for an E43 andesite shows a typical flat-topped Nelungaloo-type pattern, and exactly parallels at expected lower levels the E42 Golden Lava REE patterns. On this basis, the E43 andesites are considered to be part of the same Nelungaloo-type Phase 1 magmatic episode as the E42 trachyandesites. The E43 dacitic/trachytic lavas with 66–67% SiO_2 are probably even more evolved counterparts of the same suite, although no REE data are available to confirm this broad correlation.

Two trachytes (one a formerly glassy lava, the other a feeder dyke to the lavas) from E42, and a trachyandesite lava from E43 have been analysed for the Nd isotopic ratios (Crawford *et al.* 2007). Initial ε_{Nd} values for these three samples, all calculated at 475 Ma, are +7.8 and +7.9 for the E42 rocks, and +8.1 for the E43 lava. These values

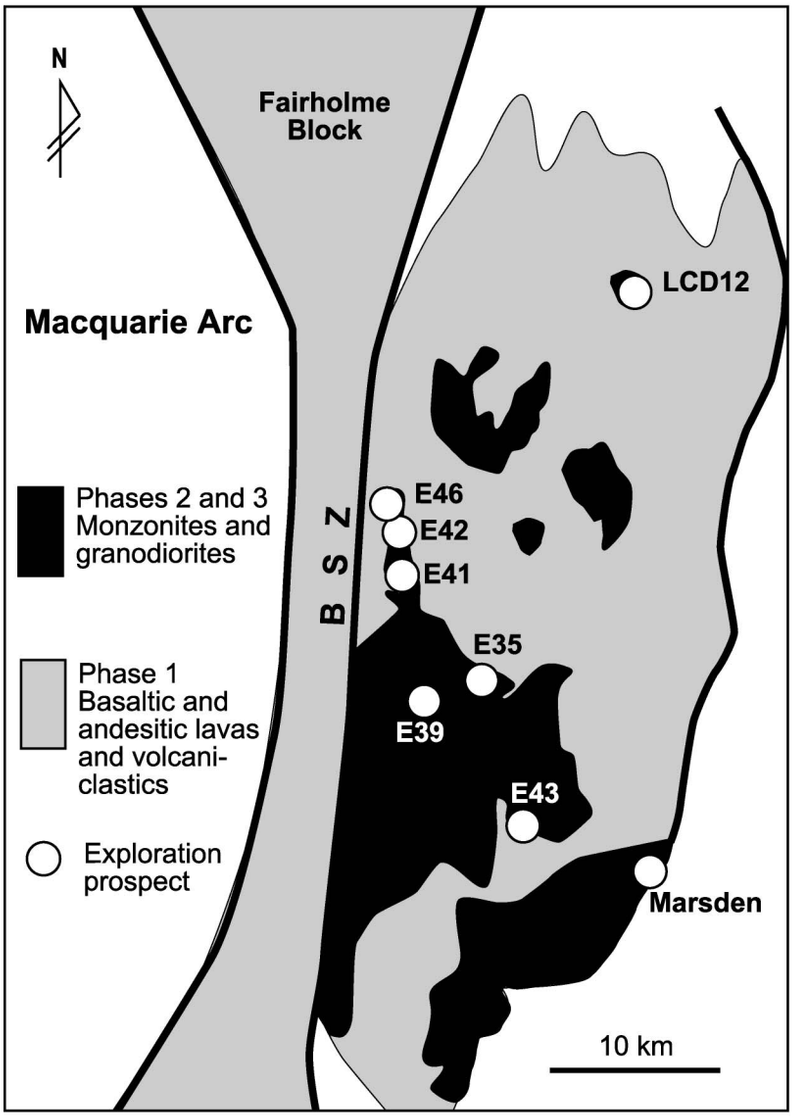

Figure 8 Generalised distribution of the Ordovician rocks and exploration prospects of the Junee–Narromine Volcanic Belt in the Cowal Igneous Complex. BSZ, Booberoi Shear Zone.

are slightly higher than data for the Nelungaloo Volcanics (+7.3 and +7.5: Crawford *et al.* 2007; Glen *et al.* 2007b) but confirm that, as for the Nelungaloo Volcanics further north in the belt, this Phase 1 magmatism in the Macquarie Arc involved no ancient crustal component, since these values are close to that of the depleted mantle in the Early Ordovician.

INTRUSIVE ROCKS

The holocrystalline intrusive rocks in the Cowal Igneous Complex show great petrographic and geochemical variation, ranging from mafic gabbros with 10–12% MgO from the Marsden drillholes, to high-level granophyric felsic intrusive rocks (granodiorites herein) with 67–76% SiO_2 from several localities. Relatively coarse-grained hornblende gabbros are well represented at Marsden, and cumulate wehrlite (olivine+clinopyroxene) and quite mafic olivine gabbro were drilled at E41. Gabbros and hornblende gabbros grade through mafic diorites to hornblende and quartz diorites or monzodiorites, with common brown to straw magmatic hornblende, not uncommon brownish biotite, and common quartz. Coarse primary sphene is present in a granodiorite from aircore hole 1504/63. Quenched marginal phases of granodioritic composition rocks contain quartz and plagioclase phenocrysts, with subordinate hornblende, and are well represented in drillholes E39/H1 and E39H3, LCD7 around 150 m, and 1504/62. K-feldspar is subordinate to plagioclase in most rocks, but occasional rocks trending to monzonitic compositions are present, and these contain both plagioclase and K-feldspar phenocrysts (e.g. in drillholes 1504/17, 1504/43, E35H1 at 9 m, E43/5 at 297 m). Apatite is most abundant in the mafic and dioritic compositions, occurring as stout prisms, whereas in felsic intrusive rocks it is usually elongate to acicular. Well-formed zircons are not uncommon in the intermediate and felsic intrusive rocks. The most distinctive difference to the MMMz suite intrusive rocks in the Narromine Igneous Complex is the relative abundance of quartz in dioritic and more evolved rocks in the Cowal Igneous Complex.

Our geochronological and geochemical study indicates that at least two major suites of intrusive rocks are

represented in the Cowal Igneous Complex, and these are very close in age and composition to those described above from the Narromine Igneous Complex. The most significant difference based on available data is that the Copper Hill Suite representatives in the Cowal Igneous Complex extend to more mafic compositions than the dacites and granodiorites in the Narromine Igneous Complex.

Drilling intersected numerous mafic dykes in the Cowal Igneous Complex, most of which transect coarser grained intrusive rocks. The dykes range from distinctive coarsely plagioclase-phyric basalts with abundant sericitised centimetre-long plagioclase phenocrysts common in E42, to aphyric basaltic to microdoleritic rocks. Clinopyroxene-phyric and aphyric basalts are present in most E43 drillholes and post-date the 447 Ma host granodiorite, suggesting correlation with Phase 4 magmatism. At Marsden, both low greenschist facies aphyric basaltic and doleritic dykes occur, as well as much fresher Ti-augite-bearing transitional alkaline dolerite dykes similar to those noted elsewhere in the Macquarie Arc and interpreted as possibly Silurian in age (Crawford *et al.* 2007).

GEOCHRONOLOGY OF COWAL IGNEOUS COMPLEX INTRUSIVE ROCKS

Using K–Ar methods, Perkins *et al.* (1995) constrained the time of intrusion of the Muddy Lake Gabbro to between 465 and 456 Ma, and showed that mineralisation-related alteration was significantly younger, around 439 Ma. Magmatic hornblende from a granodiorite at E39 was also dated by the same technique and gave an age of 465.7 ± 1 Ma (Perkins *et al.* 1995), although SHRIMP U–Pb zircon dating for the same sample yielded an age of 450.9 ± 4.5 Ma (Bastrakov 1998). The latter author also recorded an $^{40}Ar-^{39}Ar$ age of 466.8 ± 1.5 Ma on E42 diorite magmatic hornblende from drillhole 1504/13, yet a SHRIMP U–Pb zircon age from the same sample yielded an age of 455.9 ± 5.6 Ma (no information was provided on the number of grains analysed to reach the age given). This discrepancy between the Ar–Ar ages and the SHRIMP zircon U–Pb ages remains unexplained.

Although more geochronological studies of carefully constrained samples are clearly warranted for the Cowal Igneous Complex, the age range for the intrusive rocks matches very well similar MMMz suite intrusive rocks in the Narromine Igneous Complex, and argues for a major regional pulse of mainly high-K magmatism in the Darriwilian (Middle Ordovician). The age of mineralisation at Cowal is remarkably close to that at Northparkes and Cadia (mainly 440–435 Ma: Bastrakov 1998; Lickfold *et al.* 2003, 2007; Forster *et al.* 2004; Crawford *et al.* 2007) for a zero porphyry trachyte dyke that transects mineralisation at E37 in the Northparkes leases). This may imply that the structurally controlled vein-type mineralisation at Cowal E42 is linked to undiscovered *ca* 440 Ma monzonite-type intrusive rocks such as those demonstrably related to the porphyry-style mineralisation at Northparkes and Cadia, or that deformation at this time as part of the Benambran Orogeny created the veins.

We have used laser ablation ICP-MS U–Pb dating of zircons to date a granodiorite from E43 H4 at 159.8 m at 447 ± 11 Ma (Table 5; Figure 9). Details of the dating technique are given in Meffre *et al.* (2007). Although this age is based on only 12 grains, these zircons show bimodal range of dates recorded in the Narromine Igneous Complex Copper Hill Suite rocks. Four zircons have ages around 445 Ma, matching the younger population in the Copper Hill Suite rocks from the Narromine Igneous Complex, those in the Molong Volcanic Belt (Crawford *et al.* 2007), and also the SHRIMP zircon ages noted above from an E39 granodiorite. The older ages range from between 474 and 459 Ma, spanning the same age range as zircons in the Narromine Igneous Complex MMMz suite.

In summary, although further dating studies are required, we interpret available data as recording two major magmatic events for intrusive rocks in the Cowal Igneous Complex, a Darriwilian episode (*ca* 465 Ma) that generated a monzogabbro–monzodiorite suite akin to that in the Narromine Igneous Complex, and a broadly Bolindian–late Eastonian (*ca* 456–445 Ma) hornblende + quartz diorite–granodiorite–porphyritic dacite suite correlated with the Copper Hill Suite rocks elsewhere in the Macquarie Arc.

GEOCHEMISTRY OF COWAL IGNEOUS COMPLEX INTRUSIVE ROCKS

Holocrystalline intrusive rocks from the Cowal Igneous Complex have been geographically grouped into four suites for the purposes of geochemical assessment and presentation. These groups, with reference to the locality map (Figure 8), are: (i) North Cowal Intrusives, all high-level intrusive K-feldspar + quartz-phyric monzogranites with distinctive, almost aplitic textures, and all come from drillhole LCD 12 and adjacent areas, indicating the presence of a distinctive, evolved monzogranite intrusive unit in this area; (ii) Marsden area intrusives comprising rocks from the eastern and southeastern side of the Cowal Igneous Complex, including Newcrest's Marsden prospect, and North's E43 prospect; (iii) a large granodiorite intrusion widespread in drilling around the E39 prospect area, south of E42 gold development; and (iv) intrusives in the E41 and E42 prospect areas that include a range of gabbroic to granodioritic and monzonitic rocks from the western side of the Cowal Igneous Complex and are best represented by samples of Muddy Lake Gabbro at E42.

Samples were carefully selected petrographically to avoid alteration, and are among the freshest rocks analysed from the Macquarie Arc. Geochemical data (representative analyses in Table 4) are compared in Figure 10 with data for the Copper Hill Suite intrusives regionally, for the Phase 4 shoshonitic Cadia and Northparkes intrusives suites, and for the Phase 2 Narromine Igneous Complex MMMz suite. Representative chondrite-normalised REE patterns are given in Figure 11.

North Cowal intrusives

The North Cowal intrusives form a separate compositional grouping from the other Cowal intrusive suites.

Table 4 Whole-rock major- and trace-element data (recalculated to 100% volatile-free) for Cowal and Fairholme Igneous Complexes intrusive holocrystalline rocks.

Sample no.	E43H5-173.5	E43H4-376.3	E42H103-214.5	E42H361-185.8	DR39-139.8	DR41-94.5	LCD12-69.5	1504/44–44	E43H2-228.1	E43H5-342.8	E43H2-337.26
	Volcanics						Intrusives				
	Cowal				Fairholme		Cowal				
	Eastern side		Western side		Boundary EL		North		Eastern side		
Easting	544153	544763	537788	537482	533753	533581	542513	542113	544413	544153	544413
Northing	6266236	6267085	6277984	6277960	6300165	6300270	6285385	6284185	6266935	6266236	6266935
SiO_2	67.57	66.45	63.43	60.78	50.15	49.76	68.98	71.04	67.40	67.04	49.96
TiO_2	0.43	0.40	0.71	0.74	0.75	0.73	0.05	0.04	0.43	0.38	0.75
Al_2O_3	14.89	15.56	15.71	16.59	13.12	13.56	17.21	16.77	15.24	15.00	18.01
Fe_2O_3	5.60	5.56	6.33	7.94	11.57	12.40	0.71	0.72	5.44	6.02	12.39
MnO	0.07	0.08	0.13	0.25	0.12	0.20	0.01	0.01	0.06	0.09	0.23
MgO	1.71	2.55	1.42	2.01	6.98	8.49	0.26	0.19	1.66	2.31	4.92
CaO	2.07	2.92	2.42	2.06	9.88	10.51	0.95	0.02	2.07	2.43	6.67
Na_2O	6.46	5.44	4.38	3.74	3.46	2.39	5.94	4.92	6.20	5.29	3.84
K_2O	0.80	0.86	4.91	5.24	1.63	1.72	5.90	6.29	1.24	1.33	2.55
P_2O_5	0.24	0.11	0.43	0.44	0.18	0.24	0.01	0.01	0.26	0.11	0.28
LOI	1.04	2.35	2.65	3.64	2.26	2.45	1.57	0.95	1.90	1.39	1.84
Ni	bdl	4	2	2	47	48	bdl	bdl	2	bdl	5
Cr	3	19	bdl	3	206	236	bdl	bdl	bdl	12	3
V	71	128	86	88	348	360	12	9	79	124	305
Sc	14	22	13	18	49	40	bdl	bdl	16	20	36
Zr	94	76	179	188	54	55	51	35	96	72	55
Nb	1	*1.84*	*6.02*	5	3	*2.42*	*4.09*	*2.51*	*2.41*	*2.77*	*2.18*
Y	20	17	29	29	16	14	2	3	23	17	20
Sr	269	370	243	243	520	459	224	79	227	397	726
Rb	12	16	27	32	43	23	49	60	14	bdl	47
Ba	185	203	857	780	170	270	1608	335	299	367	920
Pb	40	*1.35*	*3.96*	6	3.4	*1.3*	*2.05*	*6.6*	*3.61*	*1.52*	*1.1*
Zn	589	32	166	408	30	58	36	24	49	–	1378
Cu	1	64	99	195	126	65	17	3	1401	–	5
La	–	*13.28*	*29.87*	–	–	*12.28*	*0.67*	*2.37*	*16.07*	*8.94*	*12.28*
Ce	–	*31.29*	*67.77*	–	–	*27.74*	*1.48*	*2.07*	*38.28*	*20.84*	*28.86*
Pr	–	*4.33*	*9.13*	–	–	*3.85*	*0.18*	*0.62*	*5.45*	*2.86*	*4.09*
Nd	–	*19.16*	*39.9*	–	–	*17.54*	*0.72*	*2.57*	*24.8*	*12.97*	*19.27*
Sm	–	*4.44*	*8.82*	–	–	*4.05*	*0.15*	*0.56*	*5.96*	*3.21*	*4.88*
Eu	–	*1.22*	*2.01*	–	–	*1.11*	*0.04*	*0.14*	*1.53*	*0.82*	*1.38*
Gd	–	*3.62*	*7.13*	–	–	*3.38*	*0.15*	*0.5*	*5.14*	*3.02*	*4.46*
Tb	–	*0.52*	*1.01*	–	–	*0.49*	*0.02*	*0.08*	*0.78*	*0.49*	*0.63*
Dy	–	*3.06*	*5.57*	–	–	*2.78*	*0.15*	*0.45*	*4.4*	*3.09*	*3.72*
Ho	–	*0.64*	*1.12*	–	–	*0.57*	*0.04*	*0.1*	*0.91*	*0.67*	*0.76*
Er	–	*1.9*	*3.1*	–	–	*1.57*	*0.11*	*0.27*	*2.6*	*2.02*	*2.2*

(*continued*)

Table 4 (*Continued*).

Sample no.	E43H5-173.5	E43H4-376.3	E42H103-214.5	E42H361-185.8	DR39-139.8	DR41-94.5	LCD12-69.5	1504/44 – 44	E43H2-228.1	E43H5-342.8	E43H2-337.26
			Volcanics						Intrusives		
			Cowal		Fairholme		Cowal				
	Eastern side		Western side		Boundary EL		North		Eastern side		
Easting	544153	544763	537788	537482	533753	533581	542513	542113	544413	544153	544413
Northing	6266236	6267085	6277984	6277960	6300165	6300270	6285385	6284185	6266935	6266236	6266935
Tm	–	*0.28*	*0.46*	–	–	*0.22*	*0.02*	*0.04*	*0.38*	*0.3*	*0.32*
Yb	–	*1.89*	*2.95*	–	–	*1.41*	*0.17*	*0.25*	*2.61*	*2.1*	*2.02*
Lu	–	*0.28*	*0.43*	–	–	*0.2*	*0.03*	*0.04*	*0.37*	*0.33*	*0.3*
Hf	–	*2.07*	*4.43*	–	–	*1.51*	*1.52*	*0.95*	*2.54*	*2.03*	*1.5*
Ta	–	*0.08*	*0.3*	–	–	*0.13*	*0.08*	*0.07*	*0.09*	*0.14*	*0.09*
Th	–	*1.35*	*3.96*	–	–	*1.57*	*0.12*	*0.14*	*1.41*	*1.35*	*1.32*
U	–	*1.44*	*2.57*	–	–	*1.07*	*0.59*	*0.45*	*1.49*	*1.12*	*0.91*

(*continued*)

These rocks are monzogranites with around 70% SiO_2, and ~6% each of K_2O and Na_2O, and very low TiO_2, MgO and Fe_2O_3; Zr levels of only 40–110 ppm imply significant prior extraction of Zr from these magmas. No age data are available from these rocks, but the shoshonitic geochemistry and compositional fields on the plots in Figure 10 suggest that they may correlate with high-level Goonumbla–Wombin–Northparkes shoshonitic intrusions, especially those high-SiO_2 intrusions around the Northparkes copper–gold field itself (Lickfold *et al.* 2007). No REE data are available for these rocks.

Marsden area and E43 intrusives

Analysed Marsden rocks include monzogabbros, monzodiorites, two quartz monzonites and a monzonite (Table 4). Data plotted on Figure 10, supported by the REE patterns (Figure 11b) for a diorite and a hornblende diorite from Marsden, suggest that most Marsden intrusives are broadly comparable with those from E42 and the Narromine Igneous Complex MMMz. The Marsden rocks we correlate with the regional Copper Hill Suite extend to lower SiO_2 compositions than those represented in the Narromine Igneous Complex. However, as for the E42 Muddy Lake Gabbro, data in Figure 10 suggest that some of the more evolved quartz diorite/quartz monzonites may be better correlated with the Copper Hill Suite. Further geochronological and geochemical studies of the Marsden rocks are required to elucidate the compositional groups and relationships represented among the intrusive rocks in this area. However, the E43 diorites have quite flat HREE patterns at significantly higher REE levels than the Copper Hill Suite rocks at similar SiO_2 levels, suggesting that they may represent a quite distinct Eastonian medium-K intrusive suite in the Macquarie Arc.

E41 and E42 areas

E41 samples examined include the most mafic rocks recognised in the Cowal Igneous Complex, these being cumulate wehrlitic (olivine–pyroxene) rocks and olivine-bearing gabbros; three monzodioritic intrusive rocks were also analysed from E41. E42 rocks analysed include mafic diorites transitional to leucogabbro compositions, and several dioritic rocks with ~61–63% SiO_2. Variation diagrams and discrimination plots (Figure 10) show that the more mafic E42 rocks have high-K calc-alkaline to shoshonitic affinities, but since age relationships preclude their correlation with Phase 4 intrusions, our preferred correlation is with the Middle Ordovician Phase 2 Narromine Igneous Complex MMMz suite, and we suggest that an age around 470–465 Ma is likely. Note, however, that several of the monzodiorites analysed from E42 plot within or close to the field for the Copper Hill Suite, implying that more than one intrusion may be present at E42. Further REE data are required to better constrain these relationships. From the vicinity of E42, a monzodiorite from aircore hole 1504/60 at 85.6 m yielded an initial ε_{Nd} value of 7.67, matching those values for other Middle Ordovician igneous rocks in the Macquarie Arc (see Crawford *et al.* 2007).

Table 4 (*Continued*).

Sample no.	ACDMN28/124.9	ACDMN27/161.0	ACDMN27/152.3	E39H2-77.0	E39H3-195.0	E42H156-294.0	E42H99-3167	E41H2-131.7	E41H2-205.1
	Intrusives								
	Cowal								
	Marsden E			Western side					
Easting	548763	549263	548763	538213	538563	537499	537684	537695	537808
Northing	6268735	6268885	6268735	6271385	6272885	6278135	6278085	6276701	6276886
SiO_2	50.31	49.18	56.59	66.29	69.12	57.60	53.31	47.55	48.10
TiO_2	0.67	0.84	0.86	0.36	0.27	0.93	0.65	0.60	0.31
Al_2O_3	13.65	19.27	17.57	16.47	15.90	15.11	18.40	5.52	22.16
Fe_2O_3	10.76	10.78	9.73	4.51	3.28	10.77	9.75	13.62	6.56
MnO	0.24	0.20	0.10	0.06	0.02	0.20	0.17	0.24	0.16
MgO	10.62	5.51	3.56	1.72	1.07	3.12	5.00	15.38	6.65
CaO	10.16	8.77	4.13	4.07	2.97	4.65	6.31	16.48	11.24
Na_2O	2.65	3.89	4.52	4.33	4.23	4.11	3.52	0.49	1.80
K_2O	0.69	1.05	2.35	2.05	3.02	3.07	2.62	0.10	2.97
P_2O_5	0.19	0.42	0.58	0.14	0.10	0.46	0.26	0.02	0.05
LOI	1.93	1.57	3.19	2.57	2.57	4.24	3.02	2.15	6.89
Ni	143	15	7	10	3	7	25	149	41
Cr	559	21	19	16	8	3	68	727	163
V	224	266	279	81	63	321	311	326	120
Sc	40	34	26	9	5	34	29	92	25
Zr	71	26	142	111	95	131	75	31	45
Nb	*6.93*	3	*5.24*	6	*5.57*	4	4	*0.99*	2
Y	21	19	20	11	8	25	15	17	7
Sr	636	1178	869	618	530	485	931	91	484
Rb	7	18	48	47	56	28	33	2	45
Ba	199	281	432	356	427	673	448	14	158
Pb	*1.65*	1	*2.58*	3.4	*4.3*	–	–	*0.97*	<1.5
Zn	109	90	54	51	60	125	105	86	48
Cu	43	92	1481	3930	2282	344	161	36	46
La	*15.13*	–	*22.54*	–	*9.5*	–	–	*3.14*	–
Ce	*40.02*	–	*52.71*	–	*18.94*	–	–	*9.53*	–
Pr	*5.99*	–	*7.24*	–	*2.31*	–	–	*1.66*	–
Nd	*27.83*	–	*31.47*	–	*9.18*	–	–	*9.07*	–
Sm	*6.44*	–	*6.99*	–	*1.89*	–	–	*2.9*	–
Eu	*1.6*	–	*1.88*	–	*0.56*	–	–	*0.72*	–
Gd	*5.28*	–	*5.57*	–	*1.59*	–	–	*3.4*	–
Tb	*0.74*	–	*0.75*	–	*0.26*	–	–	*0.51*	–
Dy	*4.11*	–	*3.95*	–	*1.52*	–	–	*3.15*	–
Ho	*0.81*	–	*0.78*	–	*0.34*	–	–	*0.66*	–
Er	*2.3*	–	*2.13*	–	*1.02*	–	–	*1.79*	–

(*continued*)

Table 4 (*Continued*).

Sample no.	ACDMN28/124.9	ACDMN27/161.0	ACDMN27/152.3	E39H2-77.0	E39H3-195.0	E42H156-294.0	E42H99-3167	E41H2-131.7	E41H2-205.1
				Intrusives					
				Cowal					
				Marsden E		Western side			
Easting	548763	549263	548763	538213	538563	537499	537684	537695	537808
Northing	6268735	6268885	6268735	6271385	6272885	6278135	6278085	6276701	6276886
Tm	*0.34*	–	*0.3*	–	*0.18*	–	–	*0.26*	–
Yb	*2.1*	–	*1.94*	–	*1.13*	–	–	*1.6*	–
Lu	*0.31*	–	*0.28*	–	*0.19*	–	–	*0.23*	–
Hf	*1.88*	–	*3.42*	–	*2.42*	–	–	*1.2*	–
Ta	*0.31*	–	*0.27*	–	*0.37*	–	–	*0.06*	–
Th	*1.04*	–	*3.98*	–	*2.18*	–	–	*0.38*	–
U	*0.58*	–	*3.11*	–	*1.98*	–	–	*0.25*	–

(*continued*)

Table 4 (*Continued*).

Sample no.	DR39-172.8	DR34-350.2	DR42-298.7	DR38-126.8
	Intrusives			
	Fairholme			
	Boundary EL			Dungarvan EL
Easting	533753	534193	533653	534383
Northing	6300165	6300005	6299975	6296650
SiO_2	57.39	55.91	54.59	53.74
TiO_2	0.47	0.75	0.74	1.00
Al_2O_3	18.21	17.48	18.11	16.73
$Fe2O_3$	5.69	8.57	9.13	9.96
MnO	0.08	0.10	0.09	0.18
MgO	2.78	3.41	3.46	4.08
CaO	4.82	4.74	5.39	8.35
Na_2O	3.50	5.29	4.56	3.51
K_2O	6.83	3.33	3.61	2.10
$P2O_5$	0.27	0.42	0.32	0.34
LOI	3.23	2.56	2.87	3.00
Ni	14	14	12	14
Cr	29	23	24	26
V	168	199	220	255
Sc	17	18	22	22
Zr	61	97	95	124
Nb	*5.67*	8	10	*15.3*
Y	14	20	19	27
Sr	704	629	519	682
Rb	86	33	39	29
Ba	743	594	537	359
Pb	*2.28*	bdl	*bdl*	*4.17*
Zn	39	47	44	116
Cu	236	14	269	115
La	*11.63*	–	–	*19.14*
Ce	*23.92*	–	–	*40.36*
Pr	*3*	–	–	*5.06*
Nd	*12.37*	–	–	*21.5*
Sm	*2.77*	–	–	*5.18*
Eu	*0.86*	–	–	*1.49*
Gd	*2.65*	–	–	*5.38*
Tb	*0.4*	–	–	*0.87*
Dy	*2.34*	–	–	*5.2*
Ho	*0.48*	–	–	*1.08*
Er	*1.42*	–	–	*3.03*
Tm	*0.21*	–	–	*0.45*
Yb	*1.35*	–	–	*2.8*
Lu	*0.21*–	–	–	*0.4*
Hf	*1.56*	–	–	*1.84*
Ta	*0.34*	–	–	*0.97*
Th	*1.64*	–	–	*2.7*
U	*1.05*	–	–	*1.11*

Trace elements in italics measured by ICP-MS, remainder and majors by XRF. bdl, below detection limit. See Appendix 1 for rock types analysed.

E39 area

Rocks drilled around E39 are dominated by medium-K calc-alkaline granodiorites that plot mainly in the fields defined by the Copper Hill Suite on the variation diagrams and discrimination plots in Figures 10. This is in concert with U–Pb zircon dates (see above) of 451 ± 4.5 Ma and 447 ± 7 Ma, indicating broadly Eastonian crystallisation ages for these intrusions. The REE pattern (Figure 11a) for an E39 granodiorite matches well those

Table 5 LA ICP-MS U–Pb dates of zircon grains in Cowal Igneous Complex diorite E43 H4 159.8 m.

Grain	$^{206}Pb/^{238}U$ age (207corr.)	$\pm1\sigma$	$^{206}Pb/^{238}U$	%rsd	Age	$\pm1\sigma$	$^{208}Pb/^{232}Th$	%rsd	Age	$\pm1\sigma$	$^{207}Pb/^{206}Pb$	%rsd	Age	$\pm1\sigma$	$^{207}Pb/^{235}U$	%rsd	Age	$\pm1\sigma$
JL2015	421	5	0.0686	1.1%	428	4.7	0.0269	3.3%	536	17	0.068	5.1%	870	106	0.668	5.6%	520	23
JL2019	423	4	0.0680	1.0%	424	4.0	0.0220	2.5%	440	11	0.056	3.1%	470	69	0.531	3.3%	433	12
JL2016	444	7	0.0722	1.6%	449	6.8	0.0263	4.1%	524	21	0.066	5.2%	794	108	0.657	5.1%	513	21
JL20111	444	4	0.0713	0.9%	444	3.8	0.0221	2.5%	442	11	0.056	3.2%	436	71	0.550	3.4%	445	12
JL2014	444	5	0.0721	1.0%	449	4.3	0.0249	3.2%	497	16	0.064	4.2%	733	88	0.626	4.2%	494	17
JL2017	447	5	0.0724	1.2%	450	5.2	0.0246	3.1%	492	15	0.063	3.6%	697	76	0.637	3.6%	500	14
JL2011	459	6	0.0739	1.2%	460	5.4	0.0255	3.3%	510	17	0.057	4.5%	491	99	0.592	4.7%	472	18
JL20112	460	6	0.0741	1.4%	461	6.0	0.0252	3.3%	502	16	0.057	4.7%	487	103	0.579	4.7%	464	18
JL2018	464	6	0.0748	1.3%	465	5.7	0.0254	3.2%	507	16	0.058	5.0%	538	110	0.598	4.8%	476	19
JL2013	465	6	0.0751	1.3%	467	5.7	0.0228	3.2%	455	14	0.059	4.6%	562	100	0.607	4.8%	481	18
JL20110	469	6	0.0757	1.4%	470	6.2	0.0218	3.1%	436	13	0.059	4.2%	569	92	0.604	4.6%	480	18
JL2012	474	7	0.0762	1.5%	473	6.6	0.0263	3.0%	526	16	0.056	4.7%	440	104	0.586	4.9%	468	18

for Copper Hill Suite rocks from the Narromine Igneous Complex (and regional Copper Hill Suite rocks).

Fairholme Igneous Complex

OCCURRENCE AND PETROGRAPHY

Presumed Ordovician volcanic rocks occur over Newcrest's former Fairholme leases, extending entirely in the subsurface northwest from the north–south trending Boobaroi Shear Zone (Figure 8). Newcrest has carried out regional shallow aircore drilling, and more restricted diamond core drilling of three exploration targets named Dungarvan, Boundary and Gateway, but no geological map of the Fairholme Igneous Complex has been compiled. Most material recovered during Newcrest's extensive aircore program over the Fairholme licence was too weathered for further study, but augite-phyric basaltic lavas were identified from drillholes ACNC162 (1 km north-northeast of Boundary) and ACNC141 (just northeast of Dungarvan). These, and the pillowed and brecciated lavas from Boundary (see below), suggest that the regional Ordovician basement here is dominated by basaltic lavas.

The Boundary prospect was the focus of about 10 diamond drillholes in which fresh rock was encountered mainly 80–90 m downhole. Our logging focussed on drillholes DR39, DR41 and DR42, and showed moderately altered olivine + clinopyroxene-phyric pillow basalts and basaltic breccias. These have been intruded by two distinctly different dyke suites, a transitional alkaline dolerite suite with a maximum dyke thickness of ~20 m, and a suite of massive porphyritic, mainly fine-grained monzodiorites <1 m to >30 m thick. The latter show significant petrographic variation, extending from microgabbro to almost granodiorite compositions. Most are prominently plagioclase + hornblende-phyric, with subordinate augite sometimes preserved, and ubiquitous small FeTi oxides. Dark transitional alkaline dolerites cut the other rock types, show distinctive pink Ti-augite and are less altered than the other Boundary rocks; they match petrographically similar dykes in the Cowal Igneous Complex, and we suggest that they may be associated with mid-Palaeozoic extensional magmatism in this region.

Dungarvan prospect includes ~12 diamond drillholes drilled into a northwest–southeast-oriented ovoid dioritic intrusion ~3 × 1 km in area. Rocks sampled from holes DR1 and DR38 varied from rather mafic diorites or leucogabbros to very well-preserved cumulate hornblende gabbros. At the third Fairholme prospect, Gateway, drillholes intersected a package of almost mylonitic quartz + sericite + chlorite + pyrite schists with poor or no textural preservation. Best-preserved samples retain textural evidence that they were originally porphyritic lavas with former phenocrysts of plagioclase and clinopyroxene.

GEOCHEMISTRY

Lavas

Four analysed pillow lavas and lava breccias from the Boundary prospect (two representative analyses in

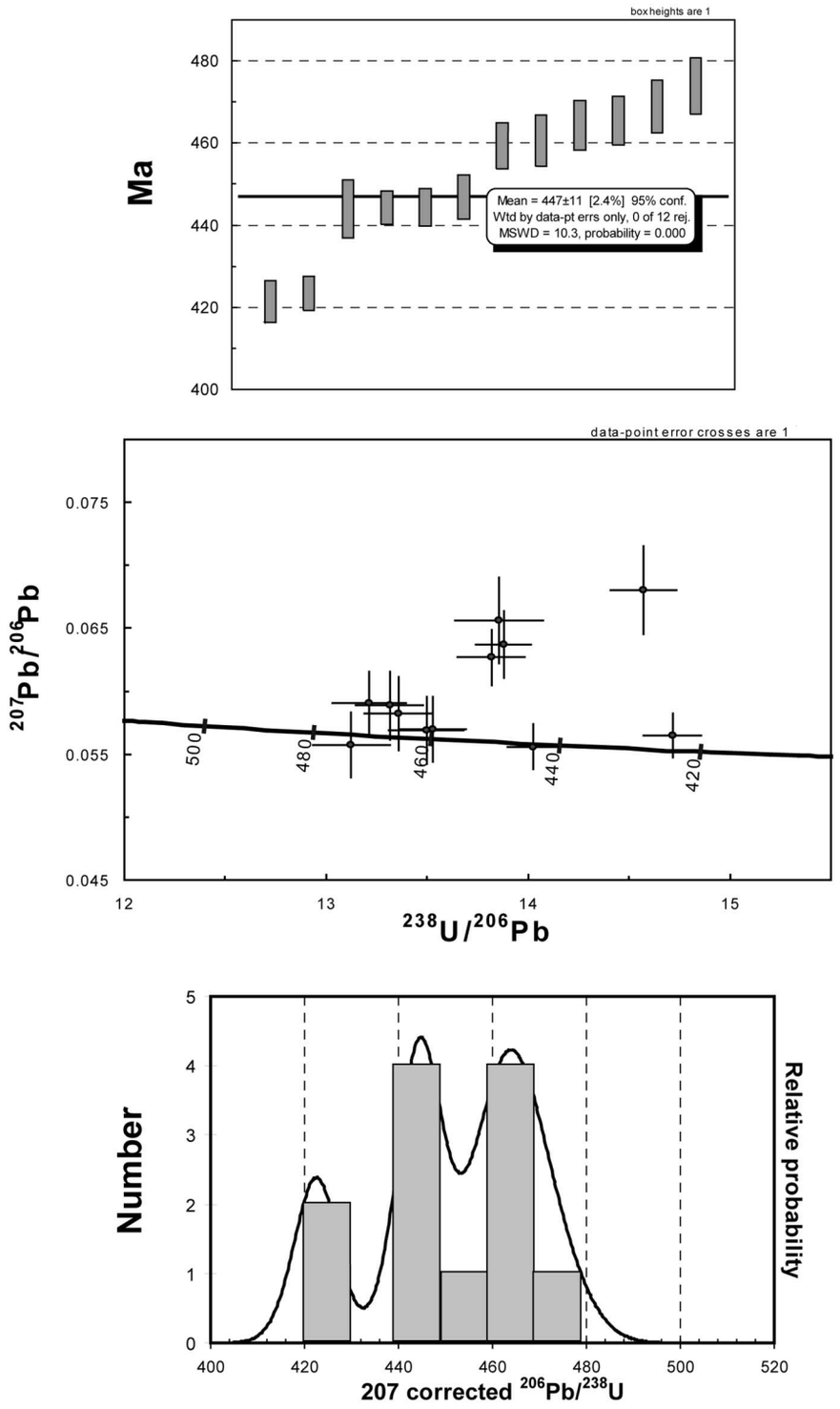

Figure 9 Data for 12 zircons from a granodiorite (drillhole E43 H4 at 159.8 m) from the Cowal Igneous Complex, determined by LA ICPMS (methodology given in Meffre *et al.* 2007). (a) Weighted mean age calculation of the $^{206}Pb/^{238}U$ ages. (b) Tera–Wasserburg concordia plot of the calibrated total $^{238}U/^{206}Pb$ ratio *vs* the total $^{207}Pb/^{206}Pb$ ratios. (c) Relative probability plot with stacked histogram of $^{206}Pb/^{238}U$ ages. As for zircons in the Phase 3 (Copper Hill Suite) rocks from the Narromine Igneous Complex, cores of grains shows ages from 474 to 460 Ma, whereas rims gives ages averaging around 445 Ma.

Table 4) define a coherent compositional group similar in most respects to the basaltic end of the Nelungaloo Volcanics range, but extending to higher MgO and lower Al_2O_3 compositions, reflecting the clinopyroxene-rich, less-evolved nature of the Boundary basalts. REE abundences for a Boundary pillow basalt (Figure 4b) define a similarly shaped REE pattern to the Phase 1 Early Ordovician Nelungaloo Volcanics, but with slightly less LREE-enrichment. We conclude that the few mafic volcanics sampled in the Fairholme Igneous Complex are more mafic on average than the Early Ordovician Nelungaloo Volcanics from further north, but with strong compositional similarities and magmatic affinities to the Nelungaloo Volcanics. On this basis, these Fairholme Igneous Complex volcanics are correlated broadly with the Nelungaloo Volcanics. No lavas with affinities to Phase 4 shoshonitic lavas have been recorded to date from the Fairholme Igneous Complex.

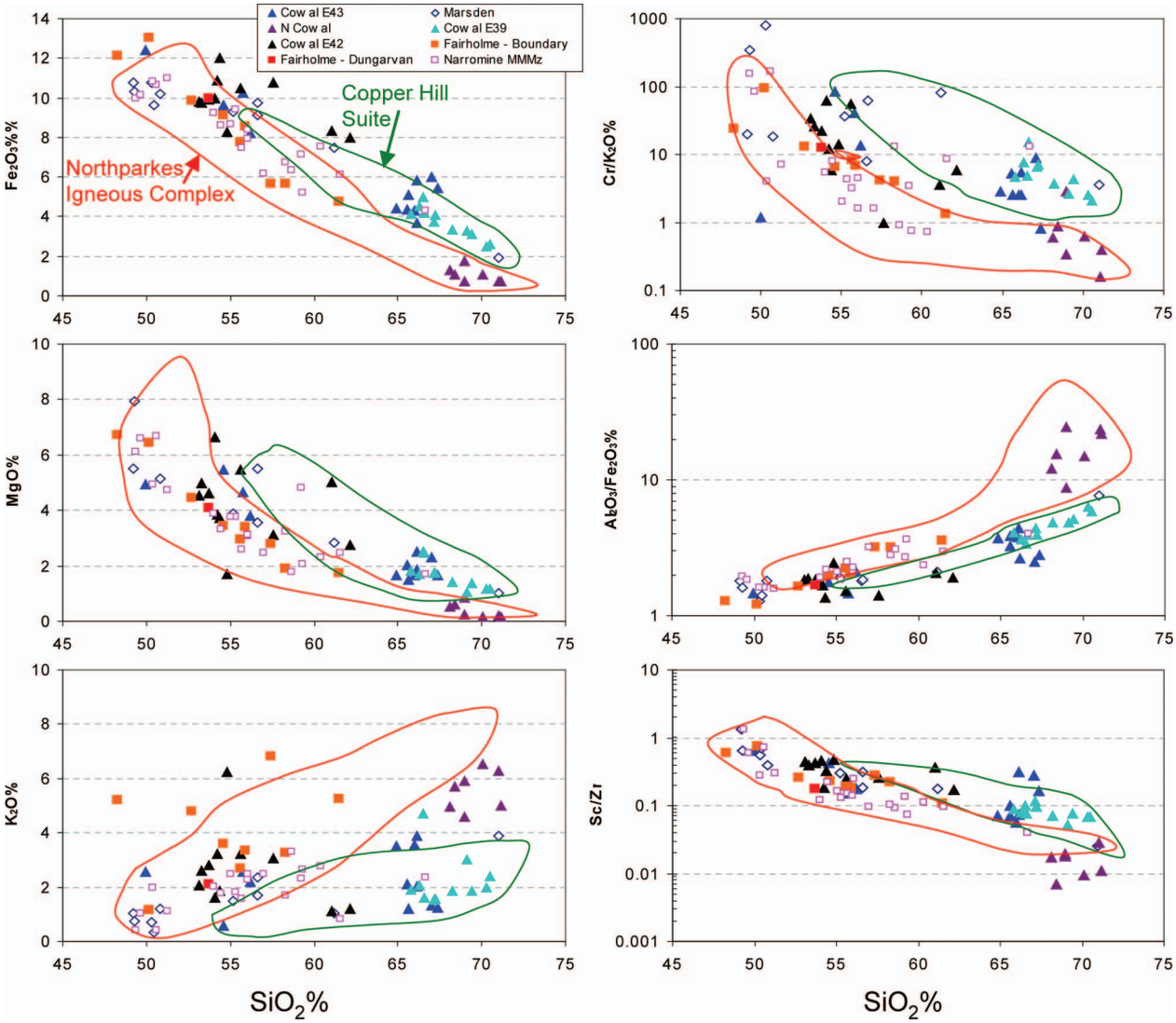

Figure 10 Major- and trace-element variation diagrams for rocks from the Cowal Igneous Complex compared with fields for intrusive rocks from the Northparkes Igneous Complex and Copper Hill Suite (data from Crawford *et al.* 2007). Also shown are data for MMMz suite intrusives from the Narromine Igneous Complex.

Intrusive rocks

Fairholme intrusives show strong compositional overlap with the shoshonitic Goonumbla – Wombin – Northparkes suite, the only notable difference being that the latter have slightly higher Zr/Nb (~15) than the Fairholme rocks (~10), reflecting very slightly higher Nb in the Fairholme suite. REE patterns for the Dungarvan and Boundary intrusives (Figure 11c) show a strong overlap with the field for Goonumbla – Wombin lavas, lacking the flattening off of the patterns between La and Nd that characterises the Boundary basaltic lavas and Nelungaloo-type patterns (Crawford *et al.* 2007). A hornblende-phyric microdiorite (intrusive latite) dyke from DR34 at Boundary has provided an age-corrected initial ε_{Nd} value of +4.74 (Glen *et al.* 2007a). This value is considerably lower than values for the Cowal Igneous Complex Early Ordovician lavas and Middle Ordovician intrusives, and is within the range of values for the Phase 4 Goonumbla – Wombin suite shoshonitic magmatism.

In summary, the intrusive rocks at Boundary in particular, but also the Dungarvan diorite, are compositionally shoshonitic, with strong similarities to the Goonumbla and Wombin Volcanics – Northparkes Igneous Complex suites. Given that the Boundary monzodiorites are high-level intrusives into Nelungaloo-

Figure 11 Chondrite-normalised REE patterns for intrusive rocks in the Cowal and Fairholme Igneous Complexes: (a) from prospect E43, compared with Copper Hill Suite intrusive rocks from Narromine, Copper Hill and Cargo; (b) from Marsden, compared with MMMz suite intrusives from the Narromine Igneous Complex; and (c) from the Boundary and Dungarvan prospects in the Fairholme Igneous Complex, showing for comparison a typical Phase 4 shoshonitic andesite from the Goonumbla Volcanics.

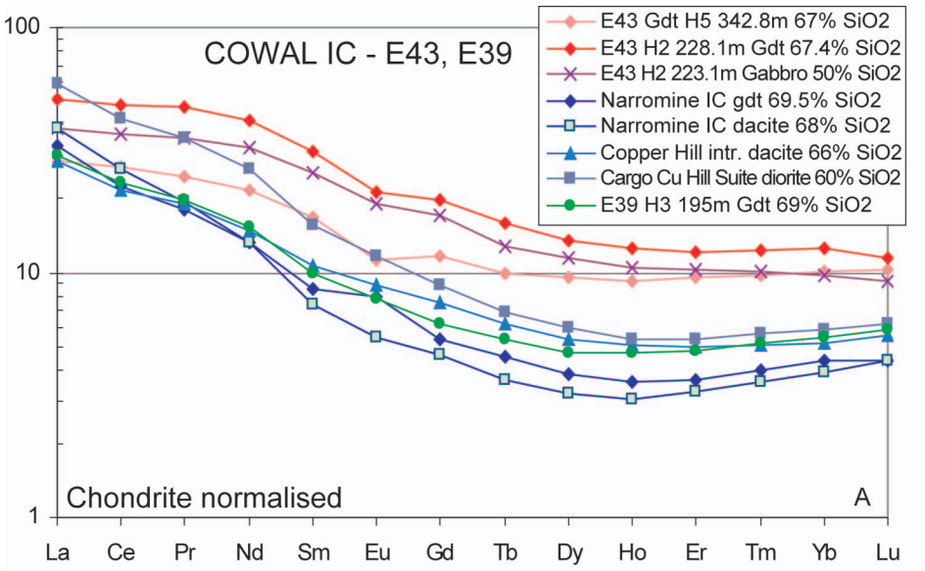
COWAL IC - E43, E39
E43 Gdt H5 342.8m 67% SiO2
E43 H2 228.1m Gdt 67.4% SiO2
E43 H2 223.1m Gabbro 50% SiO2
Narromine IC gdt 69.5% SiO2
Narromine IC dacite 68% SiO2
Copper Hill intr. dacite 66% SiO2
Cargo Cu Hill Suite diorite 60% SiO2
E39 H3 195m Gdt 69% SiO2
100
10
1
Chondrite normalised
A
La Ce Pr Nd Sm Eu Gd Tb Dy Ho Er Tm Yb Lu

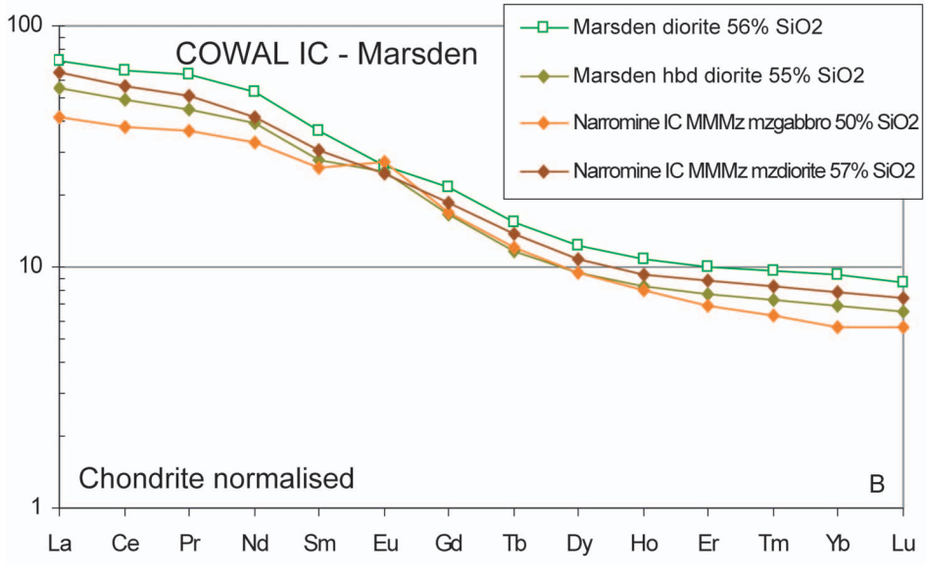
COWAL IC - Marsden
Marsden diorite 56% SiO2
Marsden hbd diorite 55% SiO2
Narromine IC MMMz mzgabbro 50% SiO2
Narromine IC MMMz mzdiorite 57% SiO2
100
10
1
Chondrite normalised
B
La Ce Pr Nd Sm Eu Gd Tb Dy Ho Er Tm Yb Lu

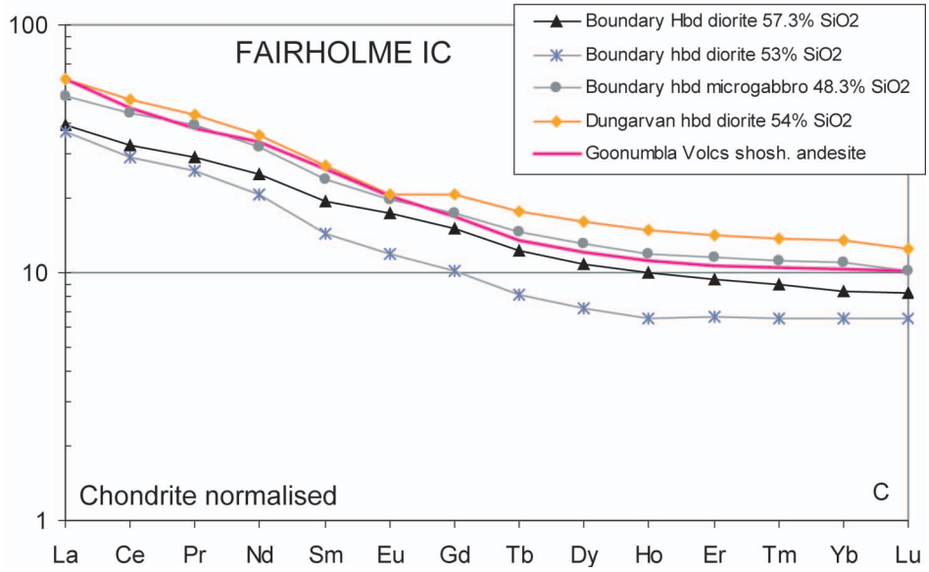
FAIRHOLME IC
Boundary Hbd diorite 57.3% SiO2
Boundary hbd diorite 53% SiO2
Boundary hbd microgabbro 48.3% SiO2
Dungarvan hbd diorite 54% SiO2
Goonumbla Volcs shosh. andesite
100
10
1
Chondrite normalised
C
La Ce Pr Nd Sm Eu Gd Tb Dy Ho Er Tm Yb Lu

type basaltic lavas, it is difficult to ignore the temporal lithogeochemical pattern similarity to the Parkes region Ordovician suites. On this basis, a Late Ordovician age might be predicted for the Boundary–Dungarvan intrusives.

DISCUSSION

Origin and significance of the Copper Hill Suite

Our studies of the distribution, timing and compositional affinities of magmatic rocks in the Macquarie Arc have shown that a widespread but relatively small-volume magmatic event, which we refer to as the Copper Hill Suite, was emplaced at *ca* 455–445 Ma, broadly corresponding with the Eastonian interval of limestone deposition and regional uplift (Crawford *et al.* 2007). Although most voluminous in the Junee–Narromine Volcanic Belt, especially in the Cowal Igneous Complex, high-level intrusive dacites and associated dioritic to granodioritic rocks are known from the Molong Volcanic Belt from the type locality at Copper Hill (Blevin 2002) and further north towards Wellington (Crawford *et al.* 2007), from the Cargo (Simpson *et al.* 2007) and Cadia (Squire & Crawford 2007) areas, and from the Rockley–Gulgong Volcanic Belt from one intrusion on Jenkins Road south of Mudgee (Crawford *et al.* 2007). Data presented by Blevin (2002) and (Crawford *et al.* 2007) demonstrate that the Copper Hill Suite has medium-K calc-alkaline affinities, with compositions extending from cumulate hornblende gabbros to granodiorite, although the average composition is probably dioritic. The abundance of hornblende in the cumulate mafic rocks suggests that they probably crystallised from andesitic rather than basaltic magmas.

The compositional range and timing of emplacement of the Copper Hill Suite deserve comment. Evidence from around Molong, and the northern end of the Cargo Block, suggests that emplacement of the stocks of porphyritic dacite and associated more holocrystalline rocks in these areas accompanied significant uplift, with widespread limestone deposition. Similarly, Copper Hill Suite rocks in the Narromine Igneous Complex show a striking textural difference between the typically medium-grained granodioritic holocrystalline intrusives, and the porphyritic dacites with very fine-grained groundmasses. From drilling, the granodiorite in the western part of the intrusive complex is at least several square kilometres in area, and in NACD8, the granodiorite occurs as a sheet at least 20 m thick with relatively coarse-grained holocrystalline margins. In contrast, in NACD83, dacite dykes compositionally identical to the granodiorite are at least 10 m thick with no textural transition from finer grained at the margins to more holocrystalline textures in the central parts of the dyke. The groundmass grainsize of the dacites indicates that these were emplaced at significantly shallower levels than the holocrystalline granodiorites, despite the almost identical geochemical compositions of these rocks. Emplacement during a period of active tectonism and uplift is indicated, and is supported by the absence of extrusive correlates of these rocks, which, if they did exist, were apparently removed by erosion before termination of Macquarie Arc magmatism.

Prior to intrusion of the Copper Hill Suite, Phase 2 magmatism in the Macquarie Arc involved a temporal transition (Crawford *et al.* 2007) from medium-K (Cargo Volcanics) and mainly high-K calc-alkaline volcanics (lower Fairbridge Volcanics, lower Blayney Volcanics), to basaltic-dominated successions with pronounced shoshonitic compositions (upper Fairbridge Volcanics, Walli Volcanics, Mt Pleasant Basalt Member, Byng Volcanics, upper Blayney Volcanics and Millthorpe Volcanics and correlates in the Rockley–Gulgong Volcanic Belt). The distinctly medium-K calc-alkaline Copper Hill Suite therefore records a departure from this trend, and reversion to magmas with lower-K affinities despite their intermediate SiO_2 contents compared with the basaltic compositions dominating the immediately preceding magmatism.

The dominance in the Copper Hill Suite of intermediate and felsic compositions with ε_{Nd} values ($>+7$: Crawford *et al.* 2007) very close to that of the Ordovician convecting upper mantle, coupled with the apparent absence of basaltic magmas in the petrogenesis of this suite, suggest that its parental magmas may have been generated by partial melting of low-K mafic rocks in the arc basement, or amphibolitic rocks in the subducting slab. Supporting the metamafic melting hypothesis, Girvan (1992) reported the presence of Mg–Al chromites with ferritchromite rims at Copper Hill, for which a restitic origin was proposed. Tectonic scenarios accommodating models for the generation of the Copper Hill Suite rocks are given in Glen *et al.* (2007a).

Zircon inheritance in felsic magmatic systems

Copper Hill Suite felsic intrusive rocks in both the Narromine and Cowal Intrusive Complexes contain zircon populations that define two distinct age groups. Cores of many grains record ages between 475 and 460 Ma, an age range matching that for the regional monzodioritic host-rocks to the Copper Hill Suite granodiorites and dacitic porphyries. Rims of these zircons record mainly Bolindian ages, around 450–441 Ma, taken to be the magmatic age of the Copper Hill Suite magmatism. There is strong evidence, therefore, that zircons from the monzodiorites and related intrusive rocks (in the Narromine Igneous Complex, the Phase 2 MMMz suite) were assimilated by the intruding Copper Hill Suite felsic magmas, and overgrown with Eastonian-age zircon. As zircon solubility is extremely temperature-sensitive, in hotter, more mafic systems, zircon inherited in this manner would be expected to dissolve, leaving little or no evidence of its former existence as xenocrysts (Watson & Harrison 1983; Miller *et al.* 2003). The Copper Hill Suite magmas have clear medium-K calc-alkaline affinities, whereas the MMMz monzodiorites and correlates intrusions in the Cowal Igneous Complex show high-K calc-alkaline affinities. Thus, the possibility that the Copper Hill Suite magmas were derived via partial melting of MMMz suite-type source rocks can be precluded. Thus, the 470–460 Ma zircon cores in Copper Hill Suite rocks cannot be

regarded as restitic (i.e. representing unmelted components of the source rock), but must have been incorporated locally in the upper crust from the immediate MMMz suite host-rocks to the Copper Hill Suite intrusions. This sounds a note of caution for the interpretation of zircon ages and their significance in I-type granitic magmatic systems.

CONCLUSIONS

More studies (particularly geochronological) are required to elucidate the time–space relationships of the Macquarie Arc rocks in the unexposed Narromine, Cowal and Fairholme Igneous Complexes. However, our data, considered within the temporal magmatic framework established for the region (Crawford *et al.* 2007), allow us to draw several important conclusions from this study.

(1) Basaltic to andesitic and trachyandesitic lavas compositionally comparable with the Phase 1 Early Ordovician Nelungaloo Volcanics are present in the Cowal, Fairholme and Narromine Igneous Complexes, and show high-K calc-alkaline compositions with depleted mantle-like ε_{Nd} values indicating no interaction of their parental magmas with continental-type crust. By implication, they probably formed in an Early Ordovician intra-oceanic arc.

(2) This volcanic and volcaniclastic basement succession was intruded by large stocks of monzogabbro–monzodiorite–monzonite in the Middle Ordovician (*ca* 465–460 Ma) that represent Macquarie Arc Phase 2 magmatism.

(3) Stocks and small intrusions representative of the Phase 3 Copper Hill Suite, ranging from hornblende gabbro to granodioritic compositions with medium-K calc-alkaline affinities, and varying texturally from relatively coarse-grained holocrystalline to porphyries with fine-grained groundmasses, were emplaced synchronously with regional-scale uplift between *ca* 455 and 441 Ma, mainly in the Bolindian–late Eastonian.

(4) In both the Fairholme Igneous Complex and the northern end of the Cowal Igneous Complex, small mainly felsic intrusions with shoshonitic affinities are interpreted to be correlates of the mainly post-Eastonian Phase 4 felsic intrusions that host porphyry Cu–Au mineralisation at Northparkes and Cadia.

ACKNOWLEDGEMENTS

This work was supported by an ARC SPIRT grant. Considerable assistance in accessing core material was provided by Bruce Mowat and Piers Reynolds (Narromine) and Stuart Smith, John Holliday and Fraser McCorcqudale (Cowal and Fairholme). We acknowledge useful input by Paul McInnes and the staff at Barrick Gold's Cowal exploration office. Phil Robinson, Sarah Gilbert and Katie McGoldrick assisted substantially with obtaining analytical data. Evgeni Bastrakov provided several whole-rock analyses and dates discussed in our study, Dick Glen provided useful comments and editorial assistance, and David Forster and Oliver Raymond made many useful points in their reviews of this paper.

REFERENCES

BASTRAKOV E. 1998. Gold mineralisation at the Lake Cowal prospect, New South Wales. PhD thesis, Australian National University, Canberra (unpubl.).

BLEVIN P. L. 2002. The petrographic and compositional character of variably K-enriched magmatic suites associated with Ordovician porphyry Cu–Au mineralisation in the Lachlan Fold Belt, Australia. *Mineralium Deposita* **37**, 87–99.

BOYNTON W. V. 1984. Geochemistry of the rare earth elements: meteorite studies. *In*: Henderson P. ed. *Rare Earth Element Geochemistry*, pp. 63–114. Elsevier, Amsterdam.

BUTERA K. M., WILLIAMS I. S., BLEVIN P. L. & SIMPSON C. J. 2001. Zircon U–Pb dating of Early Palaeozoic monzonitic intrusives from the Goonumbla area, New South Wales. *Australian Journal of Earth Sciences* **48**, 457–464.

BYWATER A., WILLIAMS S., MCINNES P. & DIJKMANS V. 2004. Developments at the Cowal gold project. *In*: Bierlien F. P. & Hough M. A. eds. *Tectonics to Mineral Discovery—Deconstructing the Lachlan Orogen*, pp. 77–82. Geological Society of Australia Abstracts **74**.

COOKE D. R., WILSON A. J., HOUSE M. J., WOLFE R. C., WALSHE J. L., LICKFOLD V. & CRAWFORD A. J. 2007. Alkalic porphyry Au–Cu and associated mineral deposits of the Ordovician to Early Silurian Macquarie Arc, New South Wales. *Australian Journal of Earth Sciences* **54**, 445–463.

CRAWFORD A. J., MEFFRE S., SQUIRE R. J., BARRON L. M. & FALLOON T. J. 2007. Middle and Late Ordovician magmatic evolution of the Macquarie Arc, Lachlan Orogen, New South Wales. *Australian Journal of Earth Sciences* **54**, 181–214.

DEFANT M. J. & DRUMMOND M. S. 1990. Derivation of some modern arc magmas by melting of young subducted lithosphere. *Nature* **347**, 662–665.

DIREEN N. G., LYONS P., KORSCH R. J. & GLEN R. A. 2001. Integrated geophysical appraisal of crustal architecture in the eastern Lachlan Orogen. *Exploration Geophysics* **32**, 252–262.

FORSTER D. A., SECCOMBE P. K. & PHILLIPS D. 2004. Controls on skarn alteration and mineralization at the Cadia deposits, New South Wales, Australia. *Economic Geology* **99**, 761–788.

GIRVAN S. W. 1992. Geology and mineralisation of the Copper Hill porphyry copper–gold deposits near Molong, New South Wales. BSc (Hons) thesis, Australian National University, Canberra, (unpubl.).

GLEN R. A., CRAWFORD A. J. & COOKE D. R. 2007a. Tectonic setting of porphyry Cu–Au mineralisation in the Ordovician–Early Silurian Macquarie Arc, Eastern Lachlan Orogen, New South Wales. *Australian Journal of Earth Sciences* **54**, 465–479.

GLEN R. A., CRAWFORD A. J., PERCIVAL I. G. & BARRON L. M. 2007b. Early Ordovician development of the Macquarie Arc, Lachlan Orogen, New South Wales. *Australian Journal of Earth Sciences* **54**, 167–179.

GLEN R. A., MEFFRE S. & SCOTT R. J. 2007c. Benambran Orogeny in the Eastern Lachlan Orogen, Australia. *Australian Journal of Earth Sciences* **54**, 385–415.

GLEN R. A., SPENCER R., WILLMORE A., DAVID V. & SCOTT R. J. 2007d. Junee–Narromine Volcanic Belt, Macquarie Arc, Lachlan Orogen, New South Wales: components and structure. *Australian Journal of Earth Sciences* **54**, 215–241.

LICKFOLD V., COOKE D. R., CRAWFORD A. J. & FANNING C. M. 2007. Shoshonitic magmatism and formation of the Northparkes porphyry Cu–Au deposits, New South Wales. *Australian Journal of Earth Sciences* **54**, 417–444.

LICKFOLD V., COOKE D. R., SMITH S. G. & ULLRICH T. D. 2003. Endeavour copper–gold porphyry deposits, Northparkes, New South Wales: intrusive history and fluid evolution. *Economic Geology* **98**, 1607–1636.

LYONS P. & WALLACE D. 1999. Geology and metallogenesis of the Parkes–Grenfell–Wyalong–Condobolin region, New South Wales. Forbes 1:250 000 Geological Sheet and Conference Guide. *Australian Geological Survey Organisation Record* **1999/20**.

MEFFRE S., SCOTT R. J., GLEN R. A. & SQUIRE R. J. 2007. Re-evaluation of contact relationships between Ordovician volcanic belts and the quartz-rich turbidites of the Lachlan Orogen. *Australian Journal of Earth Sciences* **54**, 363–383.

MILES I. N. & BROOKER M. R. 1998. Endeavour 42 deposit, Lake Cowal, New South Wales: a structurally controlled gold deposit. *Australian Journal of Earth Sciences* **45**, 837–847.

MILLER C. F., MCDOWELL S. M. & MAPES R. W. 2003. Hot and cold granites? Implications of zircon saturation temperatures and preservation of inheritance. *Geology* **31**, 529–532.

PERCIVAL I. G. & GLEN R. A. 2007. Ordovician to earliest Silurian history of the Macquarie Arc, Lachlan Orogen, New South Wales. *Australian Journal of Earth Sciences* **54**, 143–165.

PERKINS C., WALSHE J. L. & MORRISON G. 1995. Metallogenic episodes of the Tasman Fold Belt system, eastern Australia. *Economic Geology* **90**, 1443–1466.

RAYMOND O. L. & SHERWIN L. 1999. *Geology of the Parkes 1:100 000 Geological Sheet 8531, Preliminary Edition*. Australian Geological Survey Organisation, Canberra and Geological Survey of New South Wales, Sydney.

SHERWIN L. 1996. *Narromine 1:250 000 Geological Sheet SI/55-3. Explanatory Notes*. Geological Survey of New South Wales, Sydney.

SIMPSON C. J., CAS R. A. F. & ARUNDELL M. C. 2005. Volcanic evolution of a long-lived Ordovician island arc province in the Parkes region of the Lachlan Fold Belt, southeastern Australia. *Australian Journal of Earth Sciences* **52**, 863–886.

SIMPSON C. J., SCOTT R. J., CRAWFORD A. J. & MEFFRE S. 2007. Volcanology, geochemistry and structure of the Ordovician Cargo Volcanics in the Cargo–Walli region, central New South Wales. *Australian Journal of Earth Sciences* **54**, 315–352.

SQUIRE R. J. & CRAWFORD A. J. 2007. Magmatic characteristics and geochronology of Ordovician igneous rocks from the Cadia–Neville region, New South Wales: implications for tectonic evolution. *Australian Journal of Earth Sciences* **54**, 293–314.

SUN S-S. & MCDONOUGH W. F. 1989. Chemical and isotopic systematics of oceanic basalts: implications for mantle composition and processes. *In*: Saunders A. D. & Norry M. J. eds. *Magmatism in the Ocean Basins*, pp. 313–345. Geological Society of London Special Publication **42**.

WATSON E. B. & HARRISON T. M. 1983. Zircon saturation revisited: temperature and composition effects in a variety of crustal magma types. *Earth and Planetary Science Letters* **64**, 295–304.

Received 1 June 2006; accepted 30 October 2006

APPENDIX 1: ROCK TYPES ANALYSED IN TABLES 1, 3, AND 4

Sample no.	Rock type
Narromine Igneous Complex: lavas and dykes (Table 1)	
NACD28-80.0	Moderately plagioclase-phyric andesite lava or narrow dyke
NACD96-96.0	Holocrystalline trachytic textured andesite dyke
NACD105-108.4	Sparsely plagioclase-phyric andesitic dyke
NACD137-110.0	Sericite–chlorite-altered andesitic lava(?) clast
NACD20-128.9	Moderately plagioclase-phyric shallow intrusive andesite
Narromine Igneous Complex: Monzogabbro–Monzodiorite–Monzonite Suite (Table 3)	
NACD68-101.4	Shallow miarolytic monzodiorite
NACD82-143.8	Coarse-grained mafic monzodiorite
NACD85-132.7	Sparsely plagioclase-phyric monzonitic shallow intrusive
NACD89-197.0	Plagioclase-phyric micromonzonite
NACD90-144.0	Greenschist facies monzogabbro
NACD90-183.8	Cumulate monzogabbro with minor altered olivine
NACD92-61.2	Greenschist facies monzogabbro
NACD129-134	Chilled margin monzogabbro
NACD105-103.4	Greenschist facies quartz diorite
NACD2-65.0	Medium-grained monzodiorite
NACD96-102.6	Medium-grained monzonite
NACD97-53.0	Coarse monzogabbro
NACD118-55.8	Medium-grained monzogabbro
NACD119-35.7	Medium-grained monzogabbro
NACD119-58.9	Low greenschist facies monzogabbro
NACD121-80.7	Finer grained gabbro or monzogabbro
NACD122-65.8	Coarse-grained monzodiorite
NACD125-64.1	Coarse-grained hornblende monzogabbro
NACD126-60.0	Medium-grained monzogabbro
NACD130-86.9	Coarser grained monzogabbro
NACD131-79.8	Coarser grained monzogabbro
NACD135-97.4	Slightly altered monzodiorite
Narromine Igneous Complex: Copper Hill Suite (Table 3)	
NACD82-120.0	Shallow intrusive rhyodacite
NACD83-116.6	Plagioclase + quartz + hornblende + FeTiox-phyric dacite
NACD83-148.4	Plagioclase + quartz + hornblende + FeTiox-phyric dacite
NACD89-137.2	Strongly plagioclase-phyric dacite with occasional quartz phenocrysts
NACD8-137.7	Slightly altered granodiorite
NACD86-129.1	Medium-grained granodiorite
NACD137-119.1	Slightly altered quartz diorite

(*continued*)

APPENDIX 1 (*Continued*).

Sample no.	Rock type
Cowal and Fairholme Igneous Complexes: Volcanics (Table 4)	
E43H5-173.5	Plagioclase + clinopyroxene + FeTiox + apatite-phyric andesite lava
E43H4-376.3	Formerly glassy lava, altered plagioclase phenocrysts, rare mafics (altered); no apatite
E42H103-214.5	Sparsely plagioclase-phyric glassy trachytic lava, common apatite
E42H361-185.8	Moderately plagioclase-phyric andesite, occasional altered augite, apatite microphenocrysts
DR39-139.8	Clinopyroxene-phyric vesicular basalt pillowed
DR41-94.5	Vesicular clinopyroxene + altered olivine-phyric basalt pillow
Cowal and Fairholme Igneous Complexes: Intrusives (Table 4)	
LCD12-69.	K-feldspar + quartz-phyric shallow intrusive granodiorite
1504/44-44	Shallow porphyritic microgranite
E43H2-228.1	Plagioclase-phyric shallow granodiorite
E43H5-342.8	Chilled margin of granodiorite
E43H2-337.2	Holocrystalline hornblende microgabbro, interstitial green biotite
ACDMN28/124.9	Hornblende gabbro
ACDMN27/161.0	Hornblende gabbro with plenty of apatite
ACDMN8/152.3	Diorite
E39H2-77.	Medium-grained granodiorite
E39H3-195.0	High-level granodiorite
E42H156-294.0	Coarse-grained monzodiorite
E42H99-316	Diorite
E41H2-131.7	Cumulate plagioclase wehrlite
E41H2-205.1	Coarse-grained gabbro
DR39-172.8	Hornblende diorite narrow dyke, no clinopyroxene, fresh hornblende, almost no apatite
DR34-350.2	Shallow intrusive hornblende + plagioclase-phyric andesite, euhedral hornblendes
DR42-298.7	Hornblende + plagioclase-phyric shallow intrusive diorite
DR38-126.8	Hornblende diorite, fresh clinopyroxene, hornblende, biotite